



Multifunctional carbon nanomaterials for diagnostic applications in infectious diseases and tumors



Yang He¹, Chenyan Hu¹, Zhijia Li, Chuan Wu, Yuanyuan Zeng, Cheng Peng^{*}

State Key Laboratory of Southwestern Chinese Medicine Resources, College of Medical Technology, Chengdu University of Traditional Chinese Medicine, Chengdu, Sichuan, 611137, China

ARTICLE INFO

Keywords:

Carbon nanotubes
Graphene
Carbon dots
Fullerenes
Diseases
Diagnosis

ABSTRACT

Infectious diseases (such as Corona Virus Disease 2019) and tumors pose a tremendous challenge to global public health. Early diagnosis of infectious diseases and tumors can lead to effective control and early intervention of the patient's condition. Over the past few decades, carbon nanomaterials (CNs) have attracted widespread attention in different scientific disciplines. In the field of biomedicine, carbon nanotubes, graphene, carbon quantum dots and fullerenes have the ability of improving the accuracy of the diagnosis by the improvement of the diagnostic approaches. Therefore, this review highlights their applications in the diagnosis of infectious diseases and tumors over the past five years. Recent advances in the field of biosensing, bioimaging, and nucleic acid amplification by such CNs are introduced and discussed, emphasizing the importance of their unique properties in infectious disease and tumor diagnosis and the challenges and opportunities that exist for future clinical applications. Although the application of CNs in the diagnosis of several diseases is still at a beginning stage, biosensors, bioimaging technologies and nucleic acid amplification technologies built on CNs represent a new generation of promising diagnostic tools that further support their potential application in infectious disease and tumor diagnosis.

1. Introduction

Human beings have been plagued by infectious diseases and tumors for the past few decades. In the 21st century, there have been successive epidemic outbreaks of viruses including severe acute respiratory syndrome coronavirus (SARS-CoV), Ebola virus, Middle East respiratory syndrome coronavirus (MERS-CoV) and severe acute respiratory syndrome coronavirus 2 (SARS-CoV-2) (the most recent) [1–3], posing a great challenge to global public health and economy. In particular, Corona Virus Disease 2019 (COVID-19), which has spread widely around the world in the last two years, has caused approximately 350 million SARS-CoV-2 infections and over 5 million deaths. Although SARS-CoV-2 is less lethal than SARS-CoV or MERS-CoV, it has a higher transmission rate [4]. Additionally, tumors are considered to be one of the most harmful diseases worldwide. According to the World Health Organization (WHO), cancer-related mortality is predicted to escalate by 70% in the next 20 years [5]. Hence, early diagnosis of infectious diseases and tumors can lead to effective control and early intervention of the patient's conditions.

Currently, the commonly used clinical diagnostic techniques in infectious diseases and tumors include enzyme-linked immunosorbent assay (ELISA), chemiluminescent immunoassay (CLIA), polymerase chain reaction (PCR) and culture for microbial isolation and identification techniques [6,7]. Despite the high clinical popularity, sensitivity and throughput of these techniques, some aspects still need to be improved. The main disadvantages of the traditional technology include the relatively low specificity, which do not meet the diagnostic requirements. In addition, traditional detection methods have high technical demands and necessitate an expensive equipment, the latter resulting in a heavy social burden to large-scale medical examinations in developing countries. Especially in the clinical detection of SARS-CoV-2, traditional detection techniques tend to be cumbersome, time-consuming [real-time fluorescence quantitative PCR (qRT-PCR)] and have low accuracy in the detection of window period (serological antibody detection). Moreover, the current clinical diagnosis usually detects biomarkers that are free in plasma or serum, which is less sensitive compared to the detection of living cells or pathogens. Because of that, the development of high-throughput, ultra-sensitive and cost-effective novel diagnostic

* Corresponding author.

E-mail address: tcmpengcheng@163.com (C. Peng).

¹ These authors contributed equally to this work.

technology has become a hot research field. The discovery of new materials and the feasibility of processing and modification make the development of detection systems using complex materials a challenging but necessary research topic for disease diagnosis.

Recent research trends strive to discover and invent new micro- and nano-materials with unique properties [8]. In particular, as a rising star, carbon nanomaterials (CNs) have quickly attracted great interest in material science and biological applications. Indeed, they have excellent physical, chemical and structural properties, such as large specific surface area, as well as high mechanical strength and electrical properties [9,10]. CNs are members of the carbon family and include carbon nanotubes (CNTs), graphene and graphene oxide (GO), carbon dots (CDs) and fullerenes. The most relevant biological applications of CNs mainly include bioimaging [11–13], fluorescent labeling of cells [14], stem cell engineering [15–17], biosensing [18–20], gene/drug delivery [21–25] and photodynamic therapy [26–28]. Accordingly, some recent studies have examined the synthesis of CNs and their applications [29,30], although they have not focused on their diagnostic applications in infectious diseases and tumors.

This review highlights the application of CNs in the diagnosis of infectious diseases and tumors in the last five years. The relevant properties of different CNs are introduced as first, such as physical properties, optical properties, and biocompatibility. Next, the promising roles of CNs as new diagnostic materials in infectious diseases and tumors are summarized. Finally, the future challenges and opportunities for the practical

application of CNs in the diagnosis of infectious diseases and tumors are discussed.

2. Carbon nanomaterials

CNs are carbon materials with a dispersive relative scale of at least one dimension less than 100 nm, mainly including carbon nanotubes (1D), graphene (2D), carbon dots (0D), fullerenes (0D), carbon felts (1D) and nanodiamonds (3D). Since the applications of carbon felts and nanodiamonds in infectious disease and oncology diagnosis is still relatively rare, in this manuscript we focus on the first four CNs. Numerous studies on CNs have been conducted in recent years, due to their excellent chemical stability, thermal conductivity, electrical conductivity and optical properties, therefore offering a wide range of applications, especially in biomedicine. Indeed, they are widely used as biosensor components, bioimaging contrast agents, and enhancers for nucleic acid amplification technology (Fig. 1).

2.1. Carbon nanotubes

CNTs are single or multi-layered seamless nanotube structures composed of carbon atoms that are classified into single-walled carbon nanotubes (SWCNTs) and multi-walled carbon nanotubes (MWCNTs) according to the number of layers of carbon atoms [31]. The carbon atoms in CNTs mainly adopt sp^2 hybridization conferring excellent

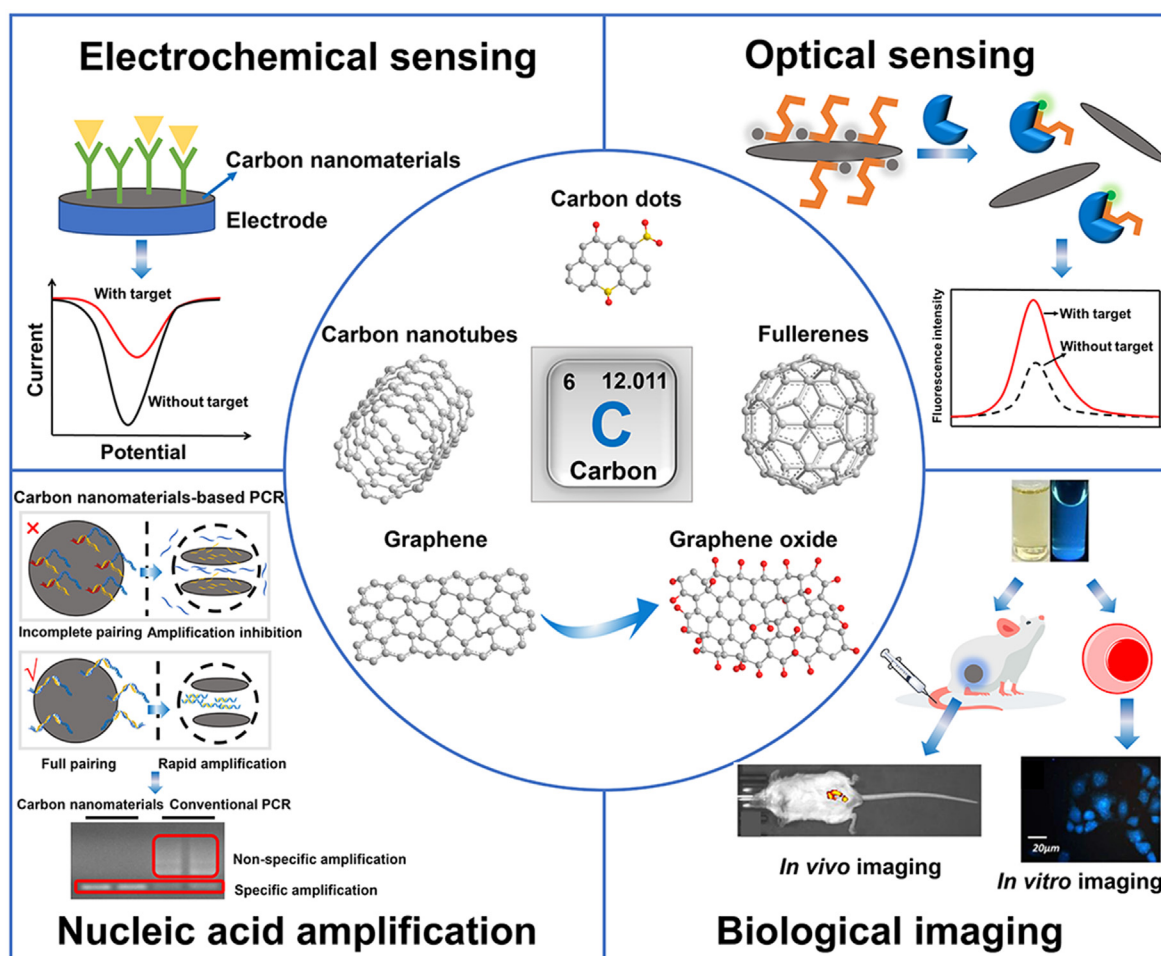


Fig. 1. Carbon nanomaterials and their various applications in disease diagnosis. Electrochemical sensing. Optical sensing. Biological imaging, reproduced with permission from Refs. [14,131,143] (Copyrights 2020, Elsevier and Royal Society of Chemistry). Nucleic acid amplification, reproduced with permission from Ref. [162] (Copyright 2021, Elsevier).

mechanical strength [32]. Besides, CNTs have promising electrical conductivity when the average wall number is close to 2.7 [33]. CNTs, when applied to disease diagnosis, generally incorporate numerous surface functional groups on the surface, including carboxyl and hydroxyl groups. Consequently, oxidized MWCNTs are chemically more active than oxidized SWCNTs, thus providing a wider range of applications. Due to the high density of oxygen-containing functional groups on the sidewalls, finely dispersed nanoparticles (NPs) can attach to the surface of MWCNTs, thus augmenting the electroactive surface area and ultimately enhancing the sensitivity of electrochemical sensors [34]. Therefore, CNTs are now widely used as components of electrochemical biosensors to obtain approaches for a sensitive and selective detection of disease-related biomarkers [35,36]. The large specific surface area of CNTs is also potentially useful in biomedicine, where a large number of metal particles [37,38], biomolecules [39–41] or other polymorphs [42, 43] can be loaded on the surface of CNTs, improving the biocompatibility of CNTs and amplifying the detection signal. The large conjugation system of CNTs can disperse the energy of the bound fluorescent dyes and thus quench the fluorescence, leading to their unique application in the construction of optical sensors. It is also noteworthy that some types of SWCNTs are able to absorb photons in the visible (400–750 nm) and near-infrared (NIR)-I (750 nm–1000 nm) windows with fluorescence in the NIR-II window (1000 nm–1700 nm) [44]. Bioimaging techniques are developed thanks to this property able to provide precious information for disease diagnosis [45,46]. Aside from the above applications, CNTs are also used in nucleic acid amplification technologies (NAAT) since they bind to single-stranded DNA (ssDNA) via π - π stacking, thus improving the amplification efficiency and enhancing the accuracy of the detection [47]. This property allows a further improvement of NAAT for the application of CNTs in disease diagnosis.

2.2. Graphene and graphene oxide

Graphene has a single-layer two-dimensional honeycomb structure formed by tightly stacked sp^2 -hybridized carbon atoms. It has received tremendous attention in biomedical fields in recent years due to its excellent electrical, optical, and chemical properties. Graphene has a remarkably large specific surface area thanks to its polyphenylene ring surface structure and can be used for the construction of biological recognition elements and delivery of drugs by binding to ssDNA and aromatic compounds via π - π stacking [48,49]. Furthermore, graphene has been extensively studied in electrochemistry since it has a carrier mobility of approximately $15,000 \text{ cm}^2/(\text{V}\cdot\text{s})$ (room temperature), exceeding the carrier mobility of silicon materials by a factor of 10 [50]. Moreover, graphene has an excellent thermal conductivity and optical properties [51,52], enabling the applications in biomedical fields.

However, despite the above-mentioned promising properties, graphene exhibits poor aqueous solubility and dissolves well only in nonpolar solvents. Therefore, numerous studies focused their attention on the enhancement of its solubility in water, and various graphene derivatives have been developed, including GO, nitrogen-doped graphene, and reduced graphene oxide (rGO), with GO as the most extensively investigated. Despite the highly conjugated surface structure of graphene is disrupted during oxidation, GO still maintains exceptional surface properties and laminar structure. The groups containing oxygen of GO enhance its chemical stability and provide a large specific surface area and modification sites. Moreover, GO has superior dispersibility in water compared to graphene [53]. The oxygen-containing groups on the GO surface can serve as attachment points for electrochemically active additives [34]. GO is currently applied in several biomedical fields, such as biosensors [54,55], bioimaging [56,57] and nucleic acid amplification [58,59]. In addition, graphitic carbon nitride (gC_3N_4), often considered as sp^2 -hybridized nitrogen-substituted graphene, has also found increasing applications in biomedical fields in recent years due to its high specific surface area and a rich variety of nanoscale multilevel structures. Due to its suitable band gap ($\sim 2.7 \text{ eV}$), gC_3N_4 aptly serves as a

component of a photoelectric sensor for biomarker determination.

Apart from acting as components of conventional electrochemical sensors, graphene and GO have been proved to exhibit field-effect transistor (FET) functionality with resistance that varies with gate voltage [60]. On the other hand, ordinary graphene and GO have a small band gap energy and lose their FET properties with little or no gate interaction. However, it has been found that doping graphene/GO with appropriate amounts of impurity elements can change their semiconductor electrical properties, leading to FET behavior with gate response [61]. Therefore, graphene/GO-based FET sensors lay the foundation for biomolecular sensing, especially for the rapid detection of SARS-CoV-2. Aside from their fluorescence quenching ability, graphene and GO have been discovered to have surface-enhanced Raman scattering (SERS), which can be utilized for disease diagnosis by amplifying the characteristic signals of biomolecules in Raman spectra. Additionally, due to the high degree of heterogeneous chemical and electronic structure of GO, some GOs exhibit strong fluorescence emission [ultraviolet (UV) to NIR region] for excellent applications in bioimaging.

2.3. Carbon dots

CDs, first discovered by Xu et al., in 2004, are novel members of the family of zero-dimensional CNs with a size less than 10 nm [62]. Generally, CDs are classified into carbon nanodots (CNDs), graphene quantum dots (GQDs), and carbon quantum dots (CQDs) according to the nature of the core structure, carbon precursor, and quantum effect, respectively [63]. CDs possess unique photoluminescence (PL) properties that distinguish them from other CNs and enable the construction of fluorescent probes for optical biosensors and bioimaging. It was confirmed that CDs with graphitic properties were identified to have visible excitation-dependent high fluorescence in the UV to NIR region. Furthermore, CDs have been reported to have two-photon and multi-photon fluorescence emission [64], enabling promising applications in multi-photon fluorescence imaging. CDs, as well as to other CNs, also have excellent electrocatalytic activity, which makes them potentially useful in the construction of electrochemical materials [65]. Furthermore, their water solubility and biocompatibility are promising thanks to the oxygen-containing functional groups (e.g., hydroxyl and carboxyl groups) that can encapsulate CDs. Compared with semiconductor quantum dots containing heavy metals, the outstanding biocompatibility and chemical inertness of CDs render them more suitable for biomedical applications. Therefore, the application of CDs in disease diagnosis has increased significantly in recent years due to these advantages. These studies explore detection techniques that are more suitable to clinical diagnosis by adjusting the chemical structure of CDs or integrating them with other nanomaterials, such as metal nanoparticles GO and CNTs.

2.4. Fullerenes

Fullerenes are common zero-dimensional carbon materials artificially created by heating graphite. Currently, buckminsterfullerene (C_{60}) and C_{70} are the most widely used fullerene materials in research. Fullerenes possess similar properties to other CNs conferring them a potential role in disease diagnosis. The surface of fullerenes can be functionalized by biorecognition molecules such as antibodies to selectively target certain biomarkers. Another distinctive photochemical property of fullerenes is the unique 18π -electron aromatic structure, which enables them to absorb photons across the solar spectrum so as to have a suitable direct band gap (2.0–2.6 eV) and a strong electron donor and acceptor capacity for photocurrent response modulation through different functionalizations. In addition, they are the most common spherical hollow molecule able to chelate heavy metals to their spherical interiors, thus significantly reducing the toxicity of contrast agents made by heavy metals and improving the safety of bioimaging techniques [66]. The water solubility and *in vivo* biocompatibility of fullerenes are pivotal issues that need to be

addressed, and numerous studies have been performed to develop fullerene materials modified with hydrophilic groups (including fullerene) to enhance their application in disease diagnosis.

3. Biosensing technology

Biosensors are devices applied for the detection and analysis of biomarker consisting of bioreceptors (including enzymes, antibodies, and aptamers), transducers (including various nanomaterials), signal amplifiers, processors, and displays [67]. The transducer converts the biochemical signal emitted by the target recognized by the bioreceptor into different types of energy, which is further amplified and processed into an output and quantifiable signal form (including electrical signal and optical signal). CNs are ideal for the storage of electrochemical energy materials and optical sensor elements due to their high electrical conductivity, large specific surface area, easy surface modification and low material cost, as well as their unique optical properties (PL or donor/acceptor intermolecular energy transfer). The application of electrochemical sensors and optical sensors constructed from CNs and used in the diagnosis of infectious diseases and tumors are discussed below.

3.1. Electrochemical technology

3.1.1. Conventional electrochemical technology

Electrochemical sensors have broad application prospects in disease diagnosis due to their miniaturization, high degree of automation, simple operation, and high sensitivity [68]. Conventional electrochemical sensors detect and quantify biomarkers by altering the surface current or electron transfer resistance (R_{et}) of the electrodes. CNs can (i) provide a biocompatible microenvironment and a large number of binding sites for molecules directed to the targets, (ii) serve as signal probe elements for the identification of specific targets, and (iii) act as transducer elements to convert the detected biochemical signals on the electrode surface into measurable electrical signals, all properties due to their large specific surface area and excellent electrical conductivity.

The commonest detection mechanism for electrochemical sensors functionalized with CNs is based on the increase/decrease of the spatial potential resistance on the electrode surface triggered by the binding of biomarkers to the recognition molecules loaded on the electrode, resulting in a further quantitative detection of the target analyte based on the change in output current (Fig. 2). Some of the conventional electrochemical sensing key researches on CNs (and their composites) for infectious disease and tumor diagnosis in the last five years are summarized in Table S1. Owing to the relatively small size and easiness of modification, one of the applications of CNs in conventional electrochemical sensors is in conjunction with signal probes as tracer tags. CNs promote the electron transfer between redox-active materials and electrode substrates, thus improving the performance of electrochemical sensors (Fig. 2a) [69]. In 2018, Chen et al. synthesized CNTs-polyaniline (PAN) nanomaterials as tracer tags that could hybridize to fragments of bulk capture probes generated after the hydrolysis of the Y-shaped structure of the target DNA/assistant probe/capture probe formed on the electrode surface [70]. This probe is formed by nicked nucleases to reduce the obstruction of the electron transfer by stem-loop capture probes, and greatly lower the R_{et} value of the electrode. The sensor allowed the quantification of the IS6110 DNA sequence specific for *Mycobacterium tuberculosis* based on the enhancement of the electrode surface current, with a detection range of 1 fM-10 nM. Furthermore, in 2021, Zhao et al. constructed redox tracer labels for SARS-CoV-2 RNA determination utilizing *p*-sulfocalix [8]arene (SCX8) functionalized graphene (SCX8-RGO) combined with toluidine blue (TB), Au, and signal probes [71]. Thanks to the abundant capture probes immobilized on the electrode surface, the redox tracer label can enhance the electrochemical response signal after

the formation of a typical sandwich structure, and the limit of detection (LOD) of the sensor for SARS-CoV-2 RNA was 3 aM. In addition, the biosensor was applied to the testing of patients with confirmed SARS-CoV-2 and revealed a higher detectable ratio than qRT-PCR. Similar studies showed that DNA/microRNA sensors with low detection limits and favorable interference resistance are also constructed by preparing probes using the composite of C_{60} with other materials such as nitrogen-doped graphene nanosheets or metalorganic framework (MOF) [72,73]. Despite the high detection specificity of electrochemical sensors with tracer tags, the sophisticated electrode modification and construction of tracer tags are both apparent drawbacks. As a result, numerous scientists are now dedicated to the rapid detection of biomarkers for the accurate diagnosis of infectious diseases and tumors by directly modifying electrodes with CNs (Fig. 2b).

For example, Zheng et al. developed a capture electrode assembled with GCE/GO/PAN/glutaraldehyde (GA)/knife bean protein A (Con A) for the specific recognition of human chronic granulocytic leukemia cancer cells (K562 cells) [74]. The resistance of the capture electrode showed a sharp increase after the recognition of K562 cells by Con A due to the dielectric behavior of the cells, and the electrode was further blocked after the incubation with the nucleic acid aptamer-DNA linker-CdTe quantum dots (QDs) probe, with a continuous reduction of the peak current of anodic stripping voltammetry (ASV). The sensor possesses a wide linear range (1.0×10^2 - 1.0×10^7 cells mL^{-1}) and a low LOD (60 cells mL^{-1}). Additionally, Jamei et al. fabricated an aptamer-based electrochemical sensor for thrombin measurement with SPCE modified with nanocomposites composed of C_{60} , MWCNTs, PEI, and polymer quantum dots (PQdot) [75]. Specific binding of thrombin to the aptamer impeded electron transfer at the electrode surface, and the sensor quantified thrombin based on the change of the current (LOD, 6 fM). However, on the other hand, the development of early diagnostic techniques for emerging outbreaks of infectious diseases (e.g., SARS-CoV-2) is disadvantageous due to the relative complexity of techniques for the preparation and purification of specific bio-recognition elements. Hussein et al. abandoned the idea of utilizing conventional antigens as capture molecules and developed a sensitive assay of SARS-CoV-2 particles with tailor-made plastic antibodies generated by molecularly imprinted polymers (MIPs) [76]. CNTs/ WO_3 were employed to modify the screen-printed electrode and intact virus particles (SARS-CoV-2 particles) were imprinted on poly(*meta*-aminophenol) (Pm-AP) polymeric films electrodeposited in situ on the electrode surface, which ultimately yielded complementary binding sites for virus pickup by washing. The decoration of CNTs/ WO_3 offered the lowest charge transfer resistance for the electrode, and the sensor allowed quantification of SARS-CoV-2 based on the increase in resistance upon virus binding (LOD, 57 $pg mL^{-1}$).

In addition, more sophisticated electrochemical sensors have been developed able of simultaneously detecting different biomarkers following composite electrochemical sensors of CNs with a single signal output. Torrente-Rodríguez et al. loaded capture antibodies or SARS-CoV-2 S1 protein on the surface of laser engraved graphene (LEG) electrodes for the detection of the viral antigen nucleocapsid protein (NP), IgM and IgG antibodies (S1-IgM and S1-IgG), and C-reactive protein (CRP) [77]. The sensor can provide information on three key aspects of SARS-CoV-2 infection: viral infection (NP), immune response (IgG and IgM) and disease severity (CRP). Besides, investigations have also been conducted using probes anchored by different redox species in CD-based electrochemical sensors for the simultaneous sensing of multiple nucleic acid biomarkers. A recent study by Pothipor et al. revealed that the designed three-screen-printed carbon electrode (3SPCE) array sensor based on the modification of gold nanoparticles (AuNPs)/GQDs/GO was able to detect miRNA-21, miRNA-155, and miRNA-210 biomarkers [78]. The dysregulation of miRNAs has been linked to the etiology of breast cancer, and studies have demonstrated that miRNAs expression profiles may be

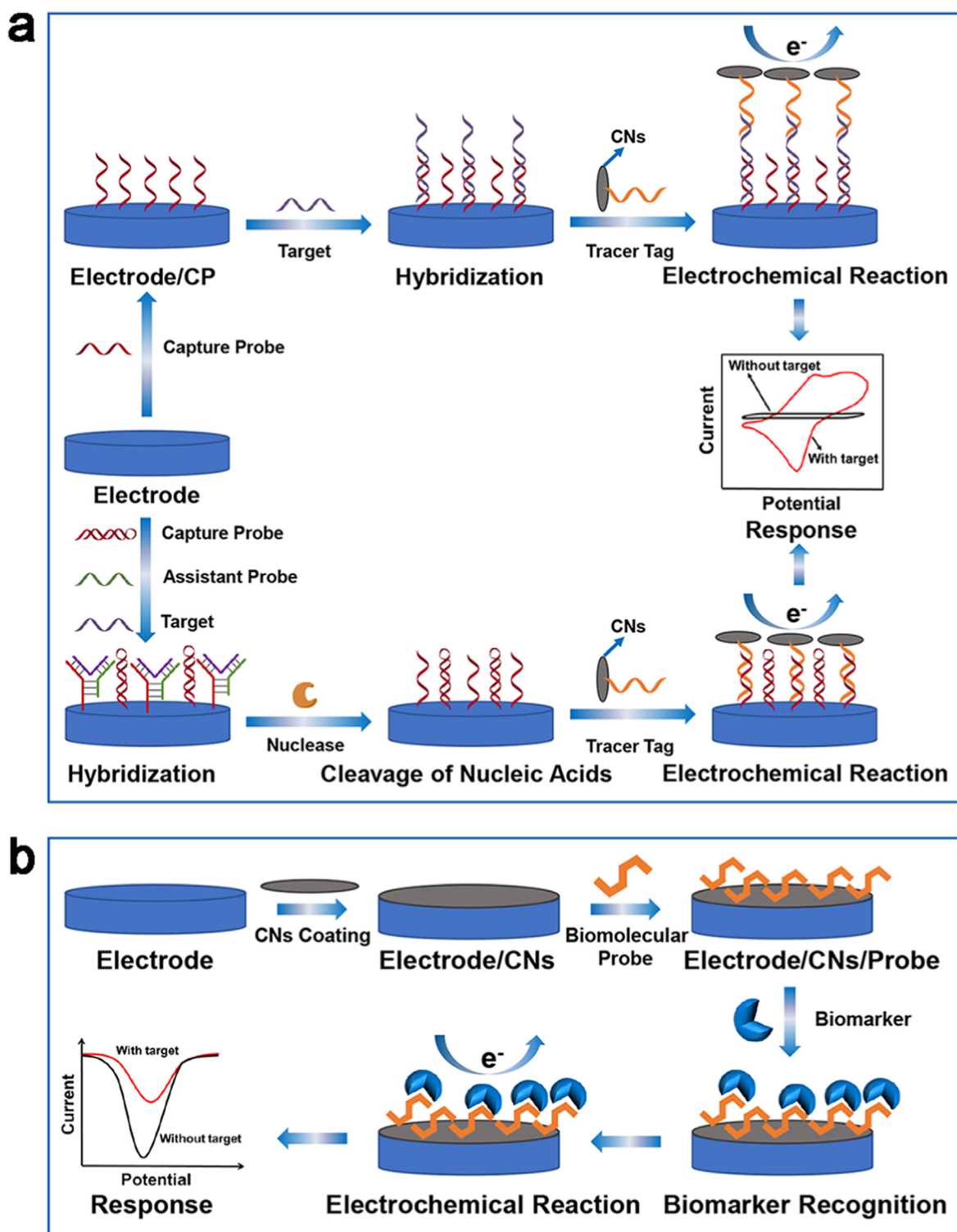


Fig. 2. Schematic presentation of conventional electrochemical biosensor for biomarker detection. (a) Schematic diagram of electrochemical biosensors with tracer tags constructed by CNs for biomarker detection. (b) Schematic presentation of electrochemical biosensors based on CN-modified electrodes for biomarker detection.

associated with tumor aggressiveness, treatment response, and patient prognosis in breast cancer [79]. In addition, these aberrantly expressed miRNAs (miRNA-21, miRNA-155, and miRNA-210) can be detected in body fluids of patients, enabling them to potentially serve as diagnostic biomarkers for breast cancer. The double-stranded structure formed by the hybridization of the target RNA with probes anchoring different redox species (anthraquinone, methylene blue and polydopamine) on the

electrode surface obstructs the transfer of electrons, resulting in a significant reduction of the peak current by differential pulse voltammetry (DPV). This assay showed LODs of 0.04 fM, 0.33 fM, and 0.28 fM for miRNA-21, miRNA-155, and miRNA-210 in human serum samples, respectively. These studies provide robust evidence that CNs have potential applications as components of electrochemical sensors that can be used in the diagnosis of infectious diseases and tumors.

3.2. Field-effect transistor technology

In recent years, FET sensors, consisting of biofunctional membranes combined with ion-sensitive field-effect transistors (ISFETs) with insulating grids, have been extensively adopted for the detection of biomarkers due to their high integration, miniaturization, high sensitivity and selectivity [80]. Among the various new materials currently available, there is a consensus that CNs are commonly used for the modification of conductive channels in FET sensors due to their high carrier mobility, extraordinary conductivity, large specific surface area and outstanding biocompatibility [81,82]. Some of the pivotal FET sensing studies on CNs (and their composites) for infectious disease and tumor diagnosis in the last five years are summarized in Table S2. Seo et al. fabricated an FET sensor for SARS-CoV-2 detection in clinical specimens by coating graphene sheets with antibodies specific for anti-SARS-CoV-2 spike protein on conductive channels (LOD, 1 fg mL^{-1}) (Fig. 3a) [83]. Furthermore, the FET sensor successfully detected SARS-CoV-2 in culture medium (LOD, $1.6 \times 10^1 \text{ pfu mL}^{-1}$) and clinical specimens (LOD, $2.42 \times 10^2 \text{ copies mL}^{-1}$). In addition to employing antibodies as capture elements, Wu et al. managed to detect HepG2 cell-derived cancerous microvesicles by immobilizing dual-aptamer on rGO sheets as capture probes (LOD, $84 \text{ particles } \mu\text{L}^{-1}$) [84]. Nevertheless, conventional single-channel FET sensors exhibit weak resistance to non-target substances in clinical assays due to the complex composition in body fluids (such as plasma, serum, saliva and urine). Accordingly, there have also been efforts to develop dual-channel FET sensors that can eliminate background interference. Hao et al. developed an intelligent aptameric dual-channel graphene-Tween 80 FET (DGTfET) to detect cytokines in body fluids to monitor the health status of patients with confirmed SARS-CoV-2 (Fig. 3b) [85]. The DGTfET biosensor, consisting of a sensing channel and a reference channel, enables the sensor to effectively minimize false response signals from unwanted background interference

in body fluids due to the differential measurement design between the two channels and the passivation layer formed by Tween 80 [86]. Thus, the DGTfET biosensor provides accurate quantification of cytokines (including interferon [IFN], interleukin [IL] and tumor necrosis factor [TNF]) in body fluids of patients with confirmed SARS-CoV-2. The FET sensor resulted in rapid quantification of IFN- γ , IL-6, and TNF- α in body fluids within 7 min with LODs of 476×10^{-15} , 611×10^{-15} , and $608 \times 10^{-15} \text{ M}$, respectively. Although CNs-based FET sensors represent a popular research direction at present, balancing portability and high accuracy of in situ biosensors is a pressing issue. There are studies exploring the development of portable FET sensor devices [87], resulting in the future application of FET sensors in clinical settings.

3.3. Photoelectrochemical technology

Approaches using the rapid and sensitive detection of biomarkers or pathogens are essential in the diagnosis of infectious diseases and tumors. Photoelectrochemical (PEC) sensing technology is a novel sensing technology that combines optics, photochemistry and electrochemistry. Photoactive materials in sensors (e.g., conducting polymers and semiconductor materials) can be excited by light signals externally applied to generate electrical signals; the target analyte directly or indirectly affects the magnitude of the electrical signal output, enabling the detection of the target analyte. PEC sensors have a low background signal and high sensitivity due to the complete separation of the two forms of energy (light and electricity) [88]. Generally, CNs are semiconductor materials with low photoelectric conversion rates due to their wide band gaps. However, their modification by materials with narrow band gaps can significantly increase the photoelectric conversion efficiency to obtain desirable PEC signals. Consequently, numerous studies focused on the construction of PEC sensors for the determination of biomarkers using modified CNs, providing promising analytical techniques for the early

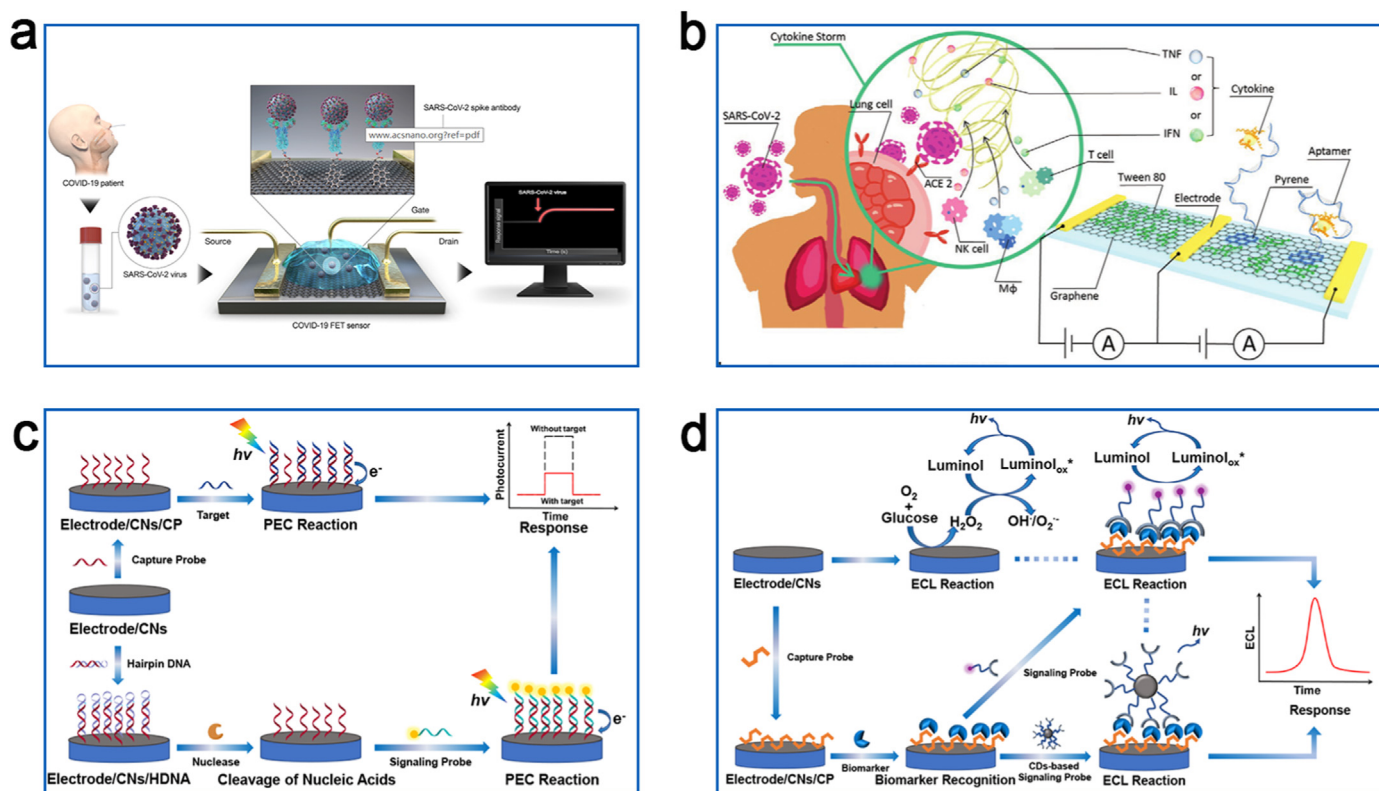


Fig. 3. Schematic illustration of FET, PEC and ECL biosensors for biomarker detection. (a) Schematic diagram of the operating procedure of a graphene-based single-channel SARS-CoV-2 FET sensor. Reproduced with permission from Ref. [83] (Copyright 2020, American Chemical Society). (b) Schematic of the principle of a graphene-based dual-channel FET sensor for the detection of SARS-CoV-2-induced cytokine storm syndrome biomarkers. Reproduced with permission from Ref. [85] (Copyright 2021, Wiley). Sensing principles of PEC (c) and ECL (d) biosensors constructed based on CNs.

diagnosis of infectious diseases and tumors (Table S2) (Fig. 3c). For example, Xue et al. proposed a “signal-off” sensor based on antimony selenide (Sb_2Se_3)-GO probes and substrates for PEC biomolecular coupling to detect the activity of DNA methyltransferase (Dam MTase) [89]. An imbalance in DNA methyltransferase activity (i.e., aberrant DNA methylation) is associated with cancer, and thus in-depth investigations of DNA methyltransferase activity can lead to valuable guidance for clinical tumor diagnosis and therapy. GO was used to increase the biocompatibility of Sb_2Se_3 and to provide more active sites for biomolecular coupling. Sb_2Se_3 -GO nanomaterials possess a significant PEC signal and can be quenched by AuNPs after the hybridization of AuNPs-functionalized DNA (S1-AuNPs) with the remaining sequence of a hairpin probe DNA (hDNA) digested by Dam MTase methylation and restriction endonuclease Dpn I and placed on the surface of the electrode. Dam MTase can be quantified based on the reduction of the photocurrent at the Sb_2Se_3 -GO modified electrode, with a LOD of the constructed PEC sensor using Dam MTase of 0.6 mU mL^{-1} . Another similar study, Meng et al. constructed a novel PEC sensor for the detection of M.SssI MTase activity, with an LOD of 0.004 U mL^{-1} using GQDs@ZIF-8 polyhedra with a large spatial site resistance as multifunctional PEC signal quencher [90].

gC_3N_4 and fullerenes are also used to construct PEC sensors. Tabrizi et al. constructed a PEC aptasensor for SARS-CoV-2 RBD detection with chitosan/cadmium sulfide (CdS)- gC_3N_4 -modified ITO electrode [91]. Visible light-driven gC_3N_4 with a band gap of 2.69 eV compensates for the high recombination rate of photogenerated electrons and holes in CdS quantum dots, while the binding of SARS-CoV-2 RBD to the aptamer in the sensor hinders the natural diffusion of ascorbic acid acting as an electron donor (PEC signal off). The PEC aptasensor can be applied for the detection of SARS-CoV-2 RBD in the range of 0.5–32.0 nM with an LOD of 0.12 nM. Additionally, Li and coworkers designed a sensor for ultrasensitive detection of adenosine triphosphate (ATP) using C_{60} modified Au nanoparticles@ MoS_2 (C_{60} -AuNP@ MoS_2) composites as signal indicators and p-type PbS QDs as signal quenchers [92]. The photoelectric conversion efficiency of C_{60} alone is low, whereas the PEC signal of the C_{60} modified by MoS_2 with a narrow band gap is significantly enhanced. Abnormal levels of ATP prompt cell damage, necrosis and apoptosis, further inducing malignant diseases such as cancer. Since ATP is involved in the cleavage of PbS QDs-labeled DNA in the sensor, the indirect detection of ATP can be achieved depending on the degree of the quenching of the PEC signal by PbS QDs (LOD, 3.30 fM). In the subsequent years, Li et al. successfully detected fragments of the P53 gene (tumor suppressor gene) and *Mycobacterium tuberculosis*-specific DNA fragments by combining C_{60} with wide-bandgap $[\text{Ru}(\text{Dcbpy})_2\text{dppz}]^{2+}$ /Rose Red dye, methylene blue, Co_3O_4 , or directly preparing fullereneol $\text{C}_{60}(\text{OH})_{25}$ with high PEC signals in PEC sensors. These sensors have an excellent sensitivity (minimum detection concentration below 1 fM) and specificity [93–96]. Although PEC sensors are simple to use and relatively inexpensive, most of the current sensors based on CNs have complex modifications and biomolecular immobilization schemes. Thus, the development of PEC sensors with simple modifications but with long-term stability and superior performance is necessary to be applied to the diagnosis of infectious diseases and tumors.

3.4. Electrochemiluminescence technology

Electrochemiluminescence (ECL) technology is another potential approach using CNs in electrochemical sensors. ECL sensors are chemiluminescent due to the luminescent substance in the system, whose luminescence is triggered by electrochemistry, allowing the quantification of the target analyte according to the luminescence intensity. ECL is highly sensitive to signal molecules loaded on the surface of the electrode due to the combination of a simple electrochemical system as well as the high intrinsic sensitivity and wide linear range of chemiluminescence. ECL sensors functionalized with CNs are extensively applied in the detection of biomarkers (Fig. 3d). An overview of some of the critical ECL

sensing studies on CNs (and their composites) for infectious disease and tumor diagnosis in the last five years is summarized in Table S2. CNs can be loaded in a large amount with adequate ECL luminescent reagents thanks to the large specific surface area and a promising biocompatibility. Besides, the 0-dimensional CDs also possess an electrically excited chemiluminescent behavior and can be used as signaling probes within the system for the accurate detection of biomarkers. Wang et al. found that MWCNTs and GQDs modified on the cathode of a carbon bipolar electrode (C-BPE) can promote some potential reduction reactions in the support channel, thereby increasing the rate of the electron transfer between the cathode and anode of C-BPE, ultimately generating a strong cathodic ECL signal in the system in the presence of luminol [97]. They also used the ECL sensor functionalized with CNs to detect glucose (tumor cell proliferation-induced glucose depletion) in samples of human serum with a minimum detection limit of 64 nM. Similarly, Bahari et al. and Wang et al. successfully detected the carbohydrate antigen 19-9 (CA19-9) (diagnostic and monitoring biomarker for tumors) and insulin (Insulinoma-induced abnormal levels of insulin) with high sensitivity and selectivity using luminol-delabeled nitrogen-doped CNDs (NCNDs) and nano- C_{60} (the nanoparticles of C_{60}) respectively, to modify the working electrode [98,99].

In addition to the modification of CNs for their use directly on the electrodes, Yang and coworkers constructed an ECL immunosensor for the detection of prostate-specific antigen (PSA) using AuNPs/GQDs-polyetherimide (PEI)-GO complexes as probes [100]. When PSA is present, a sandwich structure composed of Ab1-GCE//PSA//Ab2-AuNP/GQDs-PEI-GO is formed. The application of a voltage to the electrode resulted in the emission of light by GQDs and PSA is quantified according to this signal (LOD, 0.44 pg mL^{-1}). A similar strategy was applied by Qin et al. who detected human chorionic gonadotropin (HCG) (promotion of tumor growth and invasion), a hormone produced by the placenta (LOD, $0.33 \text{ }\mu\text{IU mL}^{-1}$), using CQDs-loaded silver nanoparticles (AgCQDs)@polymer nanospheres (PNS)-PEI nanocomplexes as ECL signaling probes [101]. Carbon nanomaterial-based ECL signaling probes can potentially detect relevant biomarkers in spiked human serum samples, indicating their potential use in the diagnosis of infectious diseases and tumors.

3.5. Optical methods

3.5.1. Colorimetric sensing technology

Colorimetric biosensors work thanks to the colorimetric reaction that generates colored compounds and allow the evaluation of the biomarker concentration by comparing or measuring the color shades of the colored solutions. The exceptionally distinctive optical properties of CNs encouraged extensive research to develop these biosensors for the detection of biomarkers. In addition, CNs have a large specific surface area, can load multiple biomolecules, and can protect biomolecules (e.g., nucleic acids or proteins) from enzymatic digestion or degradation by the environment [102,103]. These properties enable the detection of numerous biomarkers, including proteins, DNA and bacteria by colorimetric biosensors based on CNs (Fig. 4a). A summary of some of the key colorimetric sensing studies on CNs (and their composites) for infectious disease and tumor diagnosis in the last five years is presented in Table S3.

Several studies focused their attention on the use of the peroxidase-like activity of CNs to catalyze the H_2O_2 -mediated oxidation of 3,3',5,5'-tetramethylbenzidine (TMB) for the absolute quantification of biomarkers according to the degree of color change of the solution (colorless to blue). Xia et al. reported the construction of a selective biosensor for exosomes consisting of the modification of SWCNTs with aptamers to enhance the microperoxidase activity of SWCNTs to further catalyze the oxidation of TMB; the aptamers leave the surface of SWCNTs after binding to the exosomal transmembrane protein CD63, resulting in a dark to light color of the solution (LOD, $5.2 \times 10^5 \text{ }\mu\text{L}^{-1}$) [104]. On the other hand, the large specific surface area of CNs allows the increase of the loading of other materials with peroxidase-like activity, such as polyoxometalates (POMs) and MnO_2 ,

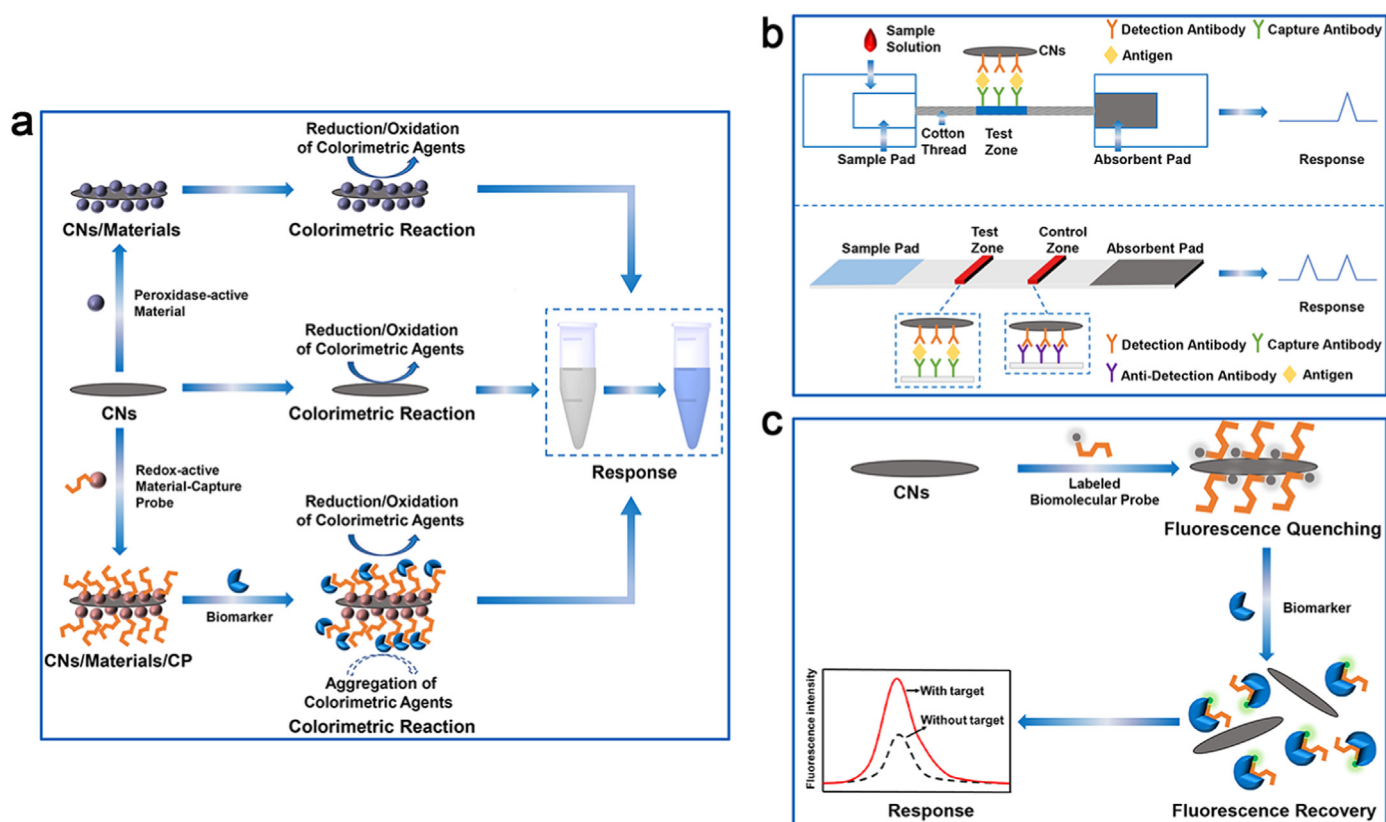


Fig. 4. Schematic representation of optical biosensors for biomarker detection. Schematic diagrams of liquid-phase colorimetric biosensors (a), immunochromatographic biosensors (b) and fluorescent biosensors (c) for biomarker detection.

to further enhance the peroxidase activity of the loaded materials for a stable, sensitive and specific detection of biomarkers [e.g., L-cysteine (abnormal levels to cause cancer) and glutathione] [105,106].

In addition to conventional TMB chromogenic solutions, Bai et al. designed a sensor for the detection of breast cancer-associated *BRCA1* gene mutation based on GO-AuNPs nanomaterials catalyzing the reduction of the colorimetric substrate 4-nitrophenol (4-NP) (bright yellow to colorless) [107]. GO offers numerous active sites in the sensor for the modification of AuNPs, further enhancing the catalytic efficiency of AuNPs for an amplification of the signal of 10^4 -fold. Gupta and coworkers developed an aptamer-GO based detection platform using the same materials (GO and AuNPs) for the detection of *Escherichia coli* (*E. coli*) [108]. The recognition of *E. coli* by the aptamer induces the aggregation of AuNPs (color of the solution: red to blue), allowing the quantitative detection of *E. coli* (LOD visible to the naked eye, 10^4 cells mL^{-1}). Unfortunately, the sensor does not work using clinical samples but only using coconut water samples, thus, this principle is a promising research field for a future development of optical sensors suitable for clinical point-of-care (POC) testing. Wei et al. developed a colorimetric and photothermal sensor for the sensitive detection of PSA according to a similar principle of the recognition of the target by aptamers, using GO-modified Fe_3O_4 NPs as signal probes [109]. The addition of PSA alters the conformation of the aptamer and triggered the detachment of GO/ Fe_3O_4 NPs from the surface of the substrate. Subsequently, the remaining Fe_3O_4 NPs in the microplate is converted to Prussian blue (PB) NPs, by mixing with potassium ferricyanide, which generated a colorful compound recognizable with the naked eye. Moreover, PB NPs induce an increase in the temperature of the immunoassay solution by NIR laser irradiation, and PSA quantification is achieved using a thermometer. The lower limit of PSA detection of the sensor is 0.31 ng mL^{-1} , which is significantly below the threshold of PSA concentration of 4.0 ng mL^{-1} for the clinical diagnosis of prostate cancer, thus meeting the clinical requirements.

Apart from the conventional liquid-phase colorimetric biosensors, colorimetric biosensors based on CNs can also be applied to immunochromatographic analysis and are usually used for the identification of biomarkers by visual inspection (Fig. 4b). Jia et al. established an assay for the rapid detection of the carcinoembryonic antigen (CEA) in the blood using a composite reporter probe of CNTs/AuNPs conjugated with specific antibodies on cotton thread [110]. Thanks to the CEA immobilized on cotton threads against specific antibodies, the CNTs/AuNP nanocomposite stacking in the test area appears as a ribbon visible with naked-eye allowing the quantification of CEA (linear range, $10\text{--}500 \text{ ng mL}^{-1}$). In addition, Meng et al. and Huang et al. constructed immunochromatographic assays for the detection of human ferritin (biomarker of anemia and tumors) and immunoglobulin IgG (biomarker of pathogenic infections) based on CNTs with a similar detection principle [111,112]. The above study revealed that the carbon nanomaterial-based colorimetric biosensor is particularly suitable for POC diagnosis in resource-limited areas thanks to its ease of use and high sensitivity.

3.5.2. Fluorescence sensing technology

Fluorescence sensing is an emerging sensing technology developed in recent years that allows the rapid and sensitive detection of biomarkers to diagnose relevant diseases. CNs have a broad absorption band overlapping the emission band of numerous photoluminescent (PL) compounds and materials, enabling them to quench the fluorescence of photoluminescent compounds and materials through the fluorescence resonance energy transfer (FRET) [113]. CNs can be versatile and efficient long-range quenchers, providing an ideal and broad platform for the design of fluorescent “OFF-ON-type” sensors (Fig. 4c) [114]. Table S3 summarizes some typical studies of fluorescent sensors using CNs (and their composites) for infectious disease and tumor diagnosis in the last five years.

The PL phenomenon of 0-dimensional CDs exists in both the visible and infrared regions [115], hence, it can be applied as fluorescent moieties to construct fluorescent sensors together with other CNs with fluorescence quenching ability. Xiang et al. developed a highly sensitive approach for the detection of CEA by combining CD-labeled specific aptamers (fluorescent probes) and azide co-functionalized GO (GO-N₃) (fluorescent inhibitors) [116]. The binding of CEA with CDs-aptamer causes the detachment of the aptamer from the GO surface, resulting in recovery of the fluorescence of CDs. This sensor detects CEA in plasma in the range of 0.01–1 ng mL⁻¹, with an LOD of 7.32 pg mL⁻¹. In addition, the use of aptamer-like recognition sensors based on CNs has been reported by several studies. Avila-Huerta et al. constructed a novel FRET-based fluorescent sensor with FITC-labeled SARS-CoV-2 spike RBD recombinant protein (F-RBD) as a signal probe for SARS-CoV-2 antibodies detection [117]. F-RBD can emit an intense fluorescence upon SARS-CoV-2 antibody detection; however, the fluorescence of F-RBD can be quenched by GO in the absence of RBD antibody. The detection limit of the sensor for SARS-CoV-2 antibody is 3 pg mL⁻¹, which satisfy the relevant requirements for its clinical application. Liu and coworkers constructed a molecular beacon (MB) probe consisting of CdSe/ZnS core-shell QDs and spherical C₆₀ to detect DNA thanks to the excellent fluorescence quenching ability of C₆₀ [118]. C₆₀-labeled oligonucleotides attached to QDs form a stem-loop structure, where C₆₀ quenches the fluorescence of QDs through FRET and charge transfer. However, the increased spacing between C₆₀ and QDs after the hybridization of the oligonucleotides with the target DNA results in the recovery of QDs fluorescence. The fluorescence intensity with each MB pre-bound to magnetic nanoparticles (MNP) enhanced by magnetic concentration allows the amplification of the detection signal by a factor of 5–10. Liu et al. constructed a fluorescent sensor for Ribonuclease H (RNase H) based on signal amplification by the hybridization chain reaction (HCR) and fluorescence quenching by GO nanosheets [119]. RNase H exerts a pivotal role in human immunodeficiency virus (HIV) viral replication, and hydrolysis of the hairpin probe H0 by RNase H induces HCR amplification between the hairpin probe H1 and the fluorescently labeled probe H2, generating a long-chain fluorescent polymer. This nanosensor offered a highly sensitive and selective platform for the detection of RNase H activity (LOD, 0.7 mU mL⁻¹).

It is also a promising modification of the system to use CNs in immunological techniques for the analysis of biomarkers based on the formation of antigen-antibody complexes. Wang et al. prepared a space-encoding microfluidic biochip to detect SARS-CoV-2 specific antigens [spike RBD protein (S antigen) and nucleocapsid protein (N antigen)] and immunoglobulin IgM/IgG antibodies [spike RBD IgG/IgM (S-IgG/S-IgM) and nucleocapsid IgG/IgM (N-IgG/N-IgM)] [120]. By microprinting specific antigens/antibodies on graphene oxide quantum dots (GOQDs)-functionalized substrates to capture the target, the chip measures the output fluorescent signal with the help of fluorescence-labeled detection antibodies or secondary antibodies that bind specifically to the target. The chip combines the advantages of GOQDs and microfluidic chips and is capable of simultaneously measuring relevant biomarkers in 60 serum specimens (LOD, 0.3 pg mL⁻¹). Another similar study of Achadu et al. shows the construction of a dual-antibody sandwich-type sensor for the quantitative detection of the influenza A virus using antibody-coupled fluorescent graphitic carbon nitride QDs (gCNQDs) as detection probes (LOD, 45 plaque forming unit (PFU) mL⁻¹) [121]. Furthermore, Xu et al. developed an ultrasensitive sensor for the measurement of SARS-CoV-2 NP with red emission-enhanced CD-based silica (RCS) spheres as fluorescent signals for lateral flow immunochromatography (LFI) [122]. The sensor has an LOD of 100 pg mL⁻¹ in the simple detection mode under UV light and 10 pg mL⁻¹ in the advanced detection mode under a fluorescence microscope. Although not all the sections of their study did not involve clinical samples or the number of clinical samples was small, contributing to less reliable experimental results, the above work demonstrated that CNs can be used as fluorescence

quenchers or fluorophores for the construction of biosensors as well as for the diagnosis of relevant diseases.

3.5.3. Surface-enhanced Raman scattering

Biosensors based on SERS are also a promising tool for the detection of biomarkers. SERS utilizes the electromagnetic field confinement effect generated by the excitation of localized surface plasmon resonance (LSPR) in specially prepared noble metal conductors or sols. The SERS signal of Raman molecules near to plasmonic nanostructures can be significantly enhanced for the label-free detection of biomarkers [123, 124]. The application of CNs in SERS sensors is actually a current research hotspot in view of the observed charge transfer induced by the chemical enhancement of SERS and superquenching of fluorescence in CNs (Table S3). El-Said et al. constructed a dual-purpose SERS and electrochemical sensor for the detection of SARS-CoV-2 spike protein employing AuNPs and reduced porous GO (rPGO) to modify the ITO electrode and as a scaffold for immobilizing anti-SARS-CoV-2 antibodies [125]. With the use of AuNPs and rPGO to enhance the Raman signals and electrochemical conductivity, the sensor exhibited LODs of 75 fM (SERS techniques) and 39.5 fM (electrochemical techniques) for SARS-CoV-2 spike protein, respectively. Pan and coworkers simultaneously synthesized a paper-based SERS (enPSERS) biosensor with an integrated enrichment ability for the sensitive, label-free detection of free bilirubin in the serum for the accurate diagnosis of jaundice and its related diseases (e.g., liver cancer) [126]. GO nanosheets have been enriched for bilirubin by strong electrostatic and π - π interactions, and the high-density plasmonic gold nanostars (GNs) on GO nanosheets provide a large number of hot spots for the bilirubin SERS signal. This allows a label-free detection of bilirubin directly from the serum (LOD, 0.436 μ M). In addition, Li et al. designed a SERS biosensor to quantify apurinic/aprimidinic endonuclease 1 (APE1) employing GO to cover Au-Cu alloys as a strategy to enhance and stabilize the SERS activity of Au-Cu alloys [127]. Since the SERS activity of AuCu/GO is regulated by the base ratio and length of the DNA sequence, this sensor allows the detection of the enzymatic activity of APE1 by the alteration of the specific Raman signal of the short DNA sequence after degradation (LOD, 1 mU mL⁻¹), which further provides information for clinical cancer screening and disease diagnosis. The GO-based sensor is able to detect biomarkers at fM concentrations, demonstrating the strong translation potential of SERS sensors constructed from CNs for their applications in clinical diagnosis.

4. Bioimaging technology

Bioimaging techniques directly inspect images of the microstructure of cells and tissues, enabling the analysis of images to investigate various physiological processes [128]. CNs are a promising platform for bioimaging applications due to their surface functionalization and extra-high specific surface area. They can be readily functionalized by nanoparticles, small molecule dyes, polymers or biomolecules to acquire specific molecular probes or contrast agents for different bioimaging applications to be further used in the detection and characterization of diseases in their early-stage. This section focuses on the application of CNs in tumors diagnosis using different molecular imaging modalities, including *in vivo* and *in vitro* fluorescence imaging, magnetic resonance imaging and other non-optical imaging techniques.

4.1. Fluorescence imaging

Fluorescence imaging is a non-invasive approach for disease diagnosis based on the photons emitted by fluorescent probes [129]. CNs with different fluorescence colors due to PL are an effect of the loaded biomolecules, doping elements (N and O) and crystal defects. Xu et al. demonstrated that curcumin-derived functionalized GO (CUDE-f-GO) composites are excellent fluorescent probes for *in vivo* and *in vitro* bioimaging. Intense fluorescent signals are identified in the cytoplasm of

CUDE-f-GO-treated MCF-7 cells and the tumor site of SW1990 tumor-bearing mice, suggesting the great potential of CUDE-f-GO composites for fluorescence imaging research. Although GO quenched part of the fluorescence of curcumin, the CUDE-f-GO complex resulted in higher bioavailability. In addition, the “bridge” linker between the fluorescent dye and GO can effectively prevent the quenching effect of GO on fluorescence. For example, Yan et al. successfully conducted fluorescence imaging of U87MG cells and tumor-bearing mice with polyethylene glycol (PEG) as a linker bridge to prevent quenching of fluorescence from GO lamellae to photosensitive substances (PSs) [130]. Furthermore, Lyu et al. found that GQDs doped with different ratios of N have diverse PL properties and are able to enter HepG2 cells through endocytosis, emitting fluorescent signals of distinct colors in the cytoplasm (Fig. 5a) [131]. Fluorescence is efficiently detected after the injection of GQDs into the mice because they are able to penetrate the skin and tissues of mice. Functional PEG₆₀₀₀/CNs with two emission wavelengths (red and green) were prepared by Fu et al. to successfully fluorescently image *Bacillus subtilis* (gram-positive), *Bacillus thuringiensis* (gram-positive), *Escherichia coli* (gram-negative) and *Pseudomonas aeruginosa* (gram-negative), indicating the potential of PEG₆₀₀₀/CNs as biocontrast agents [132]. However, commonly available CNs with down-conversion fluorescence (visible region) have a limited detection depth when applied to

bioimaging, preventing the precise localization of the lesion site. Thus, CNs that fluoresce in the NIR region have been developed for *in vitro* and *in vivo* fluorescence imaging. The NIR region consists mainly of the NIR-I window (750 nm–1000 nm) and the NIR-II window (1000 nm–1700 nm). In particular, light in the NIR-II region has low absorption and can penetrate deep into the body with weak scattering by biomolecules. For example, Yudasaka et al. introduced a SWCNTs-phospholipid polyethylene glycol (PLPEG) complex whose fluorescence is in the NIR-II region for the imaging of the whole-body vascular network in fasted mice, revealing that the increased vascular permeability in the brown adipose tissue (BAT) of fasted mice allows a remarkable accumulation of the SWCNTs-PLPEG complex in BAT [133]. Besides, Dai et al. reported a high-pressure carbon monoxide conversion (HiPCO)-based SWCNTs for NIR-IIb area fluorescence imaging of mouse blood vessels and tumors (excitation wavelength, 808 nm; fluorescence wavelength, 1500–1700 nm) (Fig. 5b) [134]. HiPCO-SWCNTs can acquire spatial resolution of ~4 mm at a maximum depth of ~3 mm and are able to accumulate significantly at the tumor site with blood circulation (half-life of ~5.6 h). Currently, CNs whose fluorescence is located in the NIR-II window suffer from high absorption, but by utilizing sufficiently bright fluorophores is an effective way to overcome the absorption effect. NIR imaging, a promising imaging technique, has not yet been applied to clinical

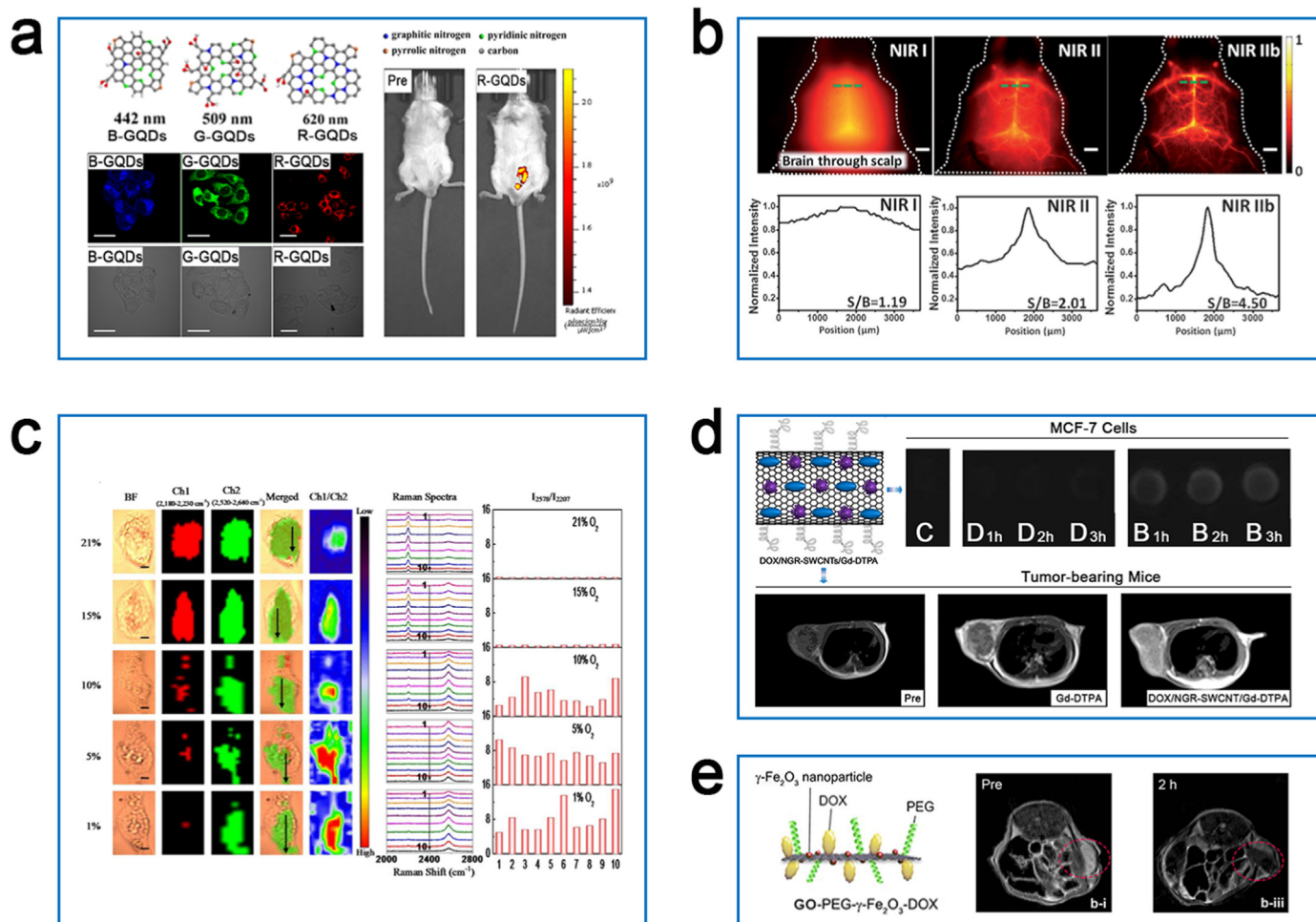


Fig. 5. Optical imaging and MRI results of CNs discussed in the review. (a) Fluorescence images of HepG2 cells and tumor-bearing mice treated with GQDs of different emission wavelengths. Reproduced with permission from Ref. [131] (Copyright 2020, Elsevier). (b) NIR fluorescence images of the cerebrovasculature of mice treated with semiconductor SWCNTs. Reproduced with permission from Ref. [134] (Copyright 2015, Wiley). (c) Raman images of HepG2 cells incubated with SWCNT/AuNPs nanoprobe at different oxygen levels. Reproduced with permission from Ref. [138] (Copyright 2019, American Chemical Society) (d) MRI of MCF-7 cells and tumor-bearing mice treated with DOX/NGR-SWCNT/Gd-DTPA. Reproduced with permission from Ref. [141] (Copyright 2016, Taylor & Francis Group). (e) MRI of H22 tumor-bearing nude mice treated with GO-PEG-γ-Fe₂O₃-DOX. The histogram demonstrates the temporal T_2 signal of the tumor site acquired by region-of-interest (ROI) analysis. Reproduced with permission from Ref. [145] (Copyright 2018, Elsevier).

diagnosis, but the development of imaging reagents with wider emission ranges and greater safety may be the direction of development to enhance NIR-II imaging capabilities.

Two-photon fluorescence imaging (TPFI) has become another promising approach in which CNs in the NIR region can be used. TPFI has promising applications in disease diagnosis due to the high signal intensity, large imaging depth, low background fluorescence, low photobleaching and weak phototoxicity [135]. The promising water solubility, fluorescence emission ability, and biocompatibility of CNs represent unique advantages in the construction of next-generation TPFI probes. Kuo and coworkers successfully achieved two-photon imaging of a human skin squamous carcinoma cell line (A431 cells) using amino-functionalized and nitrogen-doped GQDs (amino-N-GQDs) [136]. Two-photon luminescence can be achieved after anti-epidermal growth factor receptor (Ab_{EGFR})-labeling of amino-N-GQDs, with an optimal z-depth of approximately 105 μm treated with amino-N-GQDs under 800 nm fs pulsed laser excitation. Luo et al. fabricated adenine-modified GQDs (A-GQDs) with two-photon green fluorescence properties and investigated their applications in cell imaging and bacterial inhibition [137]. A-GQDs were capable of being internalized by human lung cancer A549 cells, resulting in a clear two-photon green fluorescent cell image observed at 750 nm excitation wavelength. In addition, A-GQDs were confirmed to exhibit white-light-activated antimicrobial properties. Despite TPFI imaging based on CNs is still in the early stage of exploration, the current study also indicates that the use of CNs as fluorescent TPFI probes is particularly suitable for *in vivo* studies of biological structures in the NIR range.

4.2. Raman imaging

Raman imaging technique utilizes inelastic vibrations of phonons from molecular vibrational excitation modes [128]. Consequently, compared with fluorescence imaging, Raman imaging has higher resolution, optical stability, signal-to-noise ratio, and multiplexing capabilities. CNs have a natural advantage as Raman tags for imaging cells and deep tissues due to their unique Raman fingerprint spectra. Qin et al. obtained enhanced SERS signals with the use of SWCNTs modified with Ag/Au alloy nanoparticles as substrates and combined them with alkyne derivatives exhibiting strong Raman signals in the acoustic region of cells (1800–2800 cm^{-1}), resulting in a successful application for imaging hypoxic HepG2 cells and tissues (Fig. 5c) [138]. Hypoxia is a feature of several diseases including cancer. Raman spectroscopy revealed that the signal intensity of hypoxia-incubated HepG2 cells in the 2180–2230 cm^{-1} channel gradually decreased with decreasing oxygen concentration, and in addition, hypoxia in liver tissue was still detectable at a penetration depth of 600 μm . In another similar work, Huth et al. prepared polymer-SWCNTs complexes with alkylated polymers and perylene bisimides (PBIs) covalently attached to SWCNTs [11]. The functionalized SWCNTs were well displayed in the cytoplasm of HeLa cells in Raman G-band mode. In addition to CNTs, GO has also been exploited for Raman imaging. Bugárová et al. coupled biotinylated M75 antibodies [highly selective for carbonic anhydrase (CA) IX] to the GO surface for Raman microscopy imaging [139]. Raman images successfully localized GO nanocarriers that cross the cell membrane during endocytosis. Although the utilization of CNs in Raman imaging currently requires complex modifications, Raman spectroscopy has rapidly become a potential research direction for studying cell and tissue imaging.

4.3. Magnetic resonance imaging

Magnetic resonance imaging (MRI) is a noninvasive diagnostic assay for the determination of the location and extent of diseased tissues without the use of ionizing radiation, broadly applied in the diagnosis of diseases in clinical practice. MRI relies on the different magnetic resonance relaxation of hydrogen nuclei among different tissues with a strong

magnetic field to produce contrast and thus imaging and analyzing the results [140]. However, the introduction of contrast agents in MRI is necessary to enhance the contrast and obtain an accurate diagnosis of diseases because of the low sensitivity and long signal acquisition time of the conventional MRI. Currently, the main MRI contrast agents commonly available in clinical practice include the T_1 contrast agent Gadolinium-diethylenetriamine pentaacetic acid (Gd-DTPA) and the T_2 contrast agent magnetic iron oxide nanoparticles (IONP). Nevertheless, these conventional contrast agents are highly toxic because of the presence of heavy metal ions and poor water solubility. The cavities and the large specific surface of the CNs can chelate heavy metal ions or increase the loading of IONP, further ameliorating the performance of MRI.

Yan et al. developed a SWCNT modified by an asparagine-glycine-arginine (NGR) peptide to optimize T_1 imaging agents to enable chemotherapy and tumor diagnosis in one by loading the anticancer drug doxorubicin (DOX) and the MRI contrast agent Gd-DTPA [141]. DOX/NGR-SWCNTs/Gd-DTPA has an excellent cell internalization, with a more pronounced contrast and positive antitumor effect than Gd-DTPA, as observed in both MCF-7 cells and tumor-bearing mice (Fig. 5d). Moghaddam et al. employed polyacrylic acid (PAA) to improve the dispersion of Gd^{3+} -CNTs in water and successfully performed MRI on porcine bone-marrow-derived mesenchymal stem cells ($r_1 = 150 \text{ mM}^{-1} \text{ s}^{-1}$) [142]. This hybrid material also has high intracellular dispersion, containing 10^{14} Gd^{3+} ions per cell. A new generation of contrast agents based on CNs in place of gadolinium (Gd) chelates or complexes have been proposed to further ameliorate the safety of the contrast agents. For example, Wang et al. proposed a single-layer boron-doped GQD (SL-BGQD) for the MRI of vital organs in C57BL/6 wild-type mice [143]. The non-significantly toxic SL-BGQD ($r_1 = 8.5 \text{ mM}^{-1} \text{ s}^{-1}$) shows a superior positive contrast than the contrast agent Gd-DTPA ($r_1 = 4.3 \text{ mM}^{-1} \text{ s}^{-1}$) during imaging and is able to cross the blood-brain barrier to image the neuro vascular system. Peng and coworkers fabricated fullerene quantum dots (FQDs)- MnO_2 nanocomposites responding to GSH levels in tumor cells for glutathione (GSH)-activatable MRI/fluorescence dual-mode imaging [144]. FQDs not only show an intense PL, but also greatly increase the Mn-based T_1 relaxation rate ($r_1 = 29.8 \text{ mM}^{-1} \text{ s}^{-1}$). In addition, FQDS- MnO_2 induces a significant contrast enhancement of the tumor sites in mice on T_1 -weighted MRI.

IONP can be loaded on the surface of CNs in large quantities due to the large specific surface of CNs, resulting in extensive studies in the use of superparamagnetic CNs/IONP hybrids as T_2 MRI contrast agents. Chen et al. prepared an *in vivo* imaging agent (GPF) based on GO, PEG and magnetic $\gamma\text{-Fe}_2\text{O}_3$ nanoparticles to perform MRI in mouse tumor tissues (Fig. 5e) [145]. GPF induces an effective T_2 shortening ($r_2 = 33.15 \text{ mM}^{-1} \text{ s}^{-1}$); the higher the GPF concentration, the darker the T_2 image. The MRI signal at the tumor site in mice reached its darkest intensity at 2 h after injection, indicating the potential of GPF as an *in vivo* bioimaging agent. Zhang et al. assembled Fe_3O_4 -CDs NPs with black phosphorus quantum dots (BPQDs) to prepare a new nanomaterial genipin [GP]-polyglutamic acid [PGA]- Fe_3O_4 -CDs@BPQDs specifically for enhancing T_2 MRI of tumors [146]. The tumor size contrast is pronounced in those mice treated with GP-PGA- Fe_3O_4 -Cd@BPQD nanoparticles (dark in T_2 -weighted MRI), and the nanoparticles have a low hemolytic activity and high cytocompatibility, suggesting the great potential of GP-PGA- Fe_3O_4 -Cd@BPQD NPs in nanobiotechnology. The fact that CNs can be potentially applied to detect the lesion site in live animal suggests an increased possibility of eventual clinical application of carbon nanomaterial-based contrast agents in MRI.

4.4. Positron emission tomography, single photon emission computed tomography, computed tomography, and photoacoustic imaging

CNs are also developed for non-optical imaging modalities apart from MRI, including positron emission tomography (PET), single photon emission computed tomography (SPECT), computed tomography (CT),

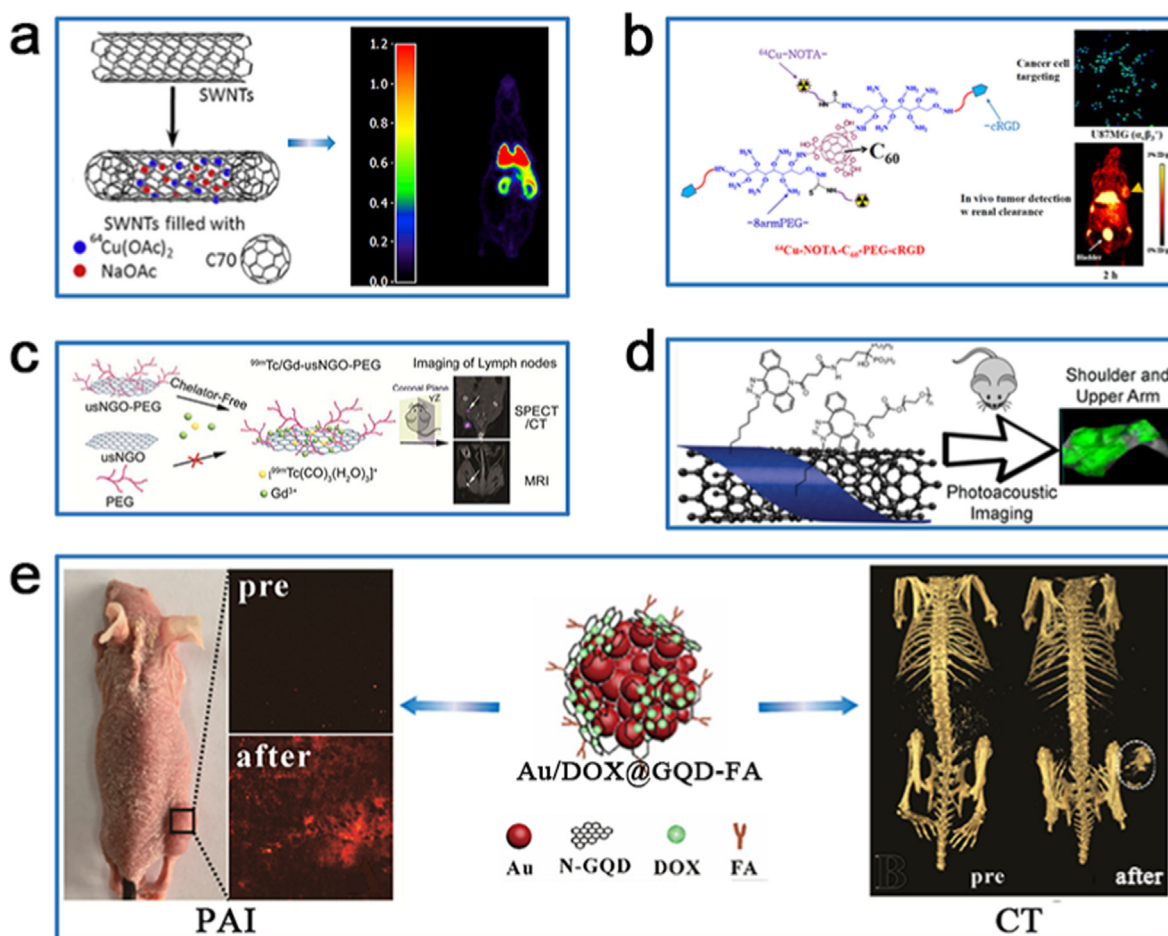


Fig. 6. The non-optical imaging results of CNs discussed in the review. (a) PET image of healthy male Wistar rats treated with $^{64}\text{Cu}@SWCNTs@β\text{-D-glucan}$. Reproduced with permission from Ref. [147] (Copyright 2017, Elsevier). (b) Fluorescence image of U87MG cells treated with fluorescein- $\text{C}_{60}\text{-PEG-cRGD}$ and PET image of U87MG tumor-bearing mice treated with $^{64}\text{Cu-NOTA-C}_{60}\text{-PEG-cRGD}$. Reproduced with permission from Ref. [148] (Copyright 2020, Elsevier). (c) SPECT/CT image and MRI of normal Balb/c mice treated with $^{99\text{m}}\text{Tc/Gd-usNGO-PEG}$. Reproduced with permission from Ref. [149] (Copyright 2017, American Chemical Society). (d) PAI of bone localization in Balb/c mice treated with SWCNTs-BP- $^{99\text{m}}\text{Tc}$. Reproduced with permission from Ref. [153] (Copyright 2020, American Chemical Society). (e) PAI and CT image of tumor site in HeLa tumor-burdened nude mice injected via Au/DOX@GQD-FA. Reproduced with permission from Ref. [155] (Copyright 2019, Elsevier).

and photoacoustic imaging (PAI), which can compensate or enhance the imaging ability of CNs for an accurate diagnosis of diseases.

PET and SPECT nuclear imaging are highly sensitive in the diagnosis of diseases since they generally use contrast agents containing radioisotopes (PET: ^{64}Cu , ^{18}F , ^{124}I , and ^{68}Ga ; SPECT: $^{99\text{m}}\text{Tc}$) [29]. Ge et al. synthesized a hybrid material consisting of ^{64}Cu -labeled SWCNTs@ $\beta\text{-D-glucan}$ ($^{64}\text{Cu}@SWCNTs@β\text{-D-glucan}$) for its use as a radiotracer for PET imaging in healthy male Wistar rats (Fig. 6a) [147]. PET imaging of $^{64}\text{Cu}@SWCNTs@β\text{-D-glucan}$ revealed that $^{64}\text{Cu}@SWCNTs@β\text{-D-glucan}$ is able to mainly localize into the lung and myocardium. In addition, PET can be combined with optical imaging. Fluorescein-functionalized $^{64}\text{Cu-C}_{60}\text{-PEG-cyclo}(\text{Arg-Gly-Asp})$ peptides (cRGD) are able to target integrin $\alpha\text{v}\beta_3$, which is involved in angiogenesis, and the biodistribution of integrin $\alpha\text{v}\beta_3$ in U87MG cells and glioblastomas in mice *in vivo* can be observed by fluorescence and PET multimodal imaging (Fig. 6b) [148]. As regard SPECT nuclear imaging, Cao et al. prepared $^{99\text{m}}\text{Tc}$ and Gd-anchored ultra-small nanographene oxide-PEG ($^{99\text{m}}\text{Tc-usNGO-PEG}$) based on a chelator-free strategy and successfully imaged lymph nodes in normal BALB/c mice *in vivo* with SPECT/CT and MRI (Fig. 6c) [149]. SPECT/CT imaging is able to detect popliteal lymph nodes, sacral lymph nodes, caudal lymph nodes and mesenteric lymph nodes in mice. Besides, $^{99\text{m}}\text{Tc-usNGO-PEG}$ in MRI also detect the aggregation in the popliteal lymph nodes.

PAI is based on laser-generated ultrasound for imaging the lesion site

by combining the high penetration depth of ultrasound imaging with the excellent contrast of fluorescence imaging [150,151]. CNTs produce acoustic waves after 500–700 nm laser excitation [152]. Genady et al. synthesized $^{99\text{m}}\text{Tc}$ radiolabeled bisphosphonate-carbon nanotube adducts (SWCNTs-BP- $^{99\text{m}}\text{Tc}$) to target regions characterized by active bone metabolism (Fig. 6d) [153]. Bisphosphonates (BPs) have a high binding affinity for hydroxyapatite (HA) at the site of bone injury or disease. The tail vein injection of SWCNTs-BP- $^{99\text{m}}\text{Tc}$ in Balb/c mice resulted in PAI displaying clear bone localization, with a rapid clearance in the blood after 1 h, demonstrating the potential of SWCNTs-BP- $^{99\text{m}}\text{Tc}$ for targeted diagnostic and drug release. Additionally, PAI can be combined with CT to obtain an ideal dual-modality imaging technique that provides spatial, positional, and distribution information of lesions in deep tissues to simultaneously obtain high-resolution pathological images and highly sensitive molecular information on the disease [154]. Xuan et al. successfully performed *in vivo* targeted PAI/CT imaging using folic acid (FA)-modified Au@GQD (Au@GQD-FA) nanoparticles in HeLa tumor-bearing nude mice (Fig. 6e) [155]. FA receptors are overexpressed on the surface of HeLa cells, and strong PA signals are observed at the tumor site after irradiation with a 744 nm laser; CT results also suggested the promising CT imaging capabilities of Au@GQD-FA nanoparticles. The research on non-optical imaging techniques based on CNs is currently limited to living animals, but these studies allow for a

continuous expansion of the diagnostic application of CN-based biomaterials to more clinical diseases.

5. Nucleic acid amplification technologies

NAAT is one of the molecular diagnostic techniques that detects nucleic acids at the single copy level based on the principle of central signal amplification, in order to diagnose human health and diseases. NAAT comprises various PCR (including conventional PCR, qRT-PCR, and digital PCR [dPCR]) and isothermal amplification techniques [including loop-mediated isothermal amplification (LAMP), recombinase polymerase amplification (RPA), and rolling circle amplification (RCA)] [156,157]. Nevertheless, conventional NAAT techniques have some limitations such as insufficient sensitivity or specificity, and the requirement of specialized and expensive instruments. Therefore, the adaptation of CNs to improve the deficiencies of the conventional NAAT may be a promising approach to improve its diagnostic efficiency. Some critical studies of NAAT on CNs (and their composites) for infectious disease and tumor diagnosis in the last five years are summarized in Table S4.

5.1. Improvement of PCR systems

PCR is a technique that mimics DNA replication *in vitro* and is one of the most used techniques in modern biomedicine. ssDNA can adsorb to the surface of CNs by various interactions of the exposed bases with CNs (including π - π stacking, hydrophobic interactions, hydrogen bonding, and van der Waals forces), while the nucleobases of dsDNA are shielded by phosphate structures with a negative charge and have a low affinity for CNs [158]. Jeong and coworkers developed a method for yield extraction of SARS-CoV-2 nucleic acids using captured ssDNA sequences attached to the surface of SWCNTs, for direct downstream detection by qRT-PCR [159]. With the complementary binding of captured ssDNA to the target and reversible aggregation of SWCNT induced under acidic conditions, viral RNA can be extracted in high yield by subsequent adjustment of solution pH. The nucleic acid extraction kit revealed approximately 80% higher extraction efficiency than the commercial silica-column kit. In addition, Wang et al. applied GO in conventional PCR and demonstrated that $1 \mu\text{g mL}^{-1}$ of GO effectively improves the specificity of error-prone multi-round PCR [160]. GO used in PCR systems promotes the formation of matched primer-template complexes, but inhibits the formation of mismatched primer-template complexes during the PCR, suggesting that the interaction between primers and GO plays an important role. The existing hypothesis suggested that GO can adsorb ssDNA (e.g. primers) through π - π stacking and hydrogen bonding, thereby allowing the matched primer-template complexes to be detached from its surface for subsequent PCR reactions, while the primers remain adsorbed on its surface when mismatched. The above findings encouraged our group to introduce in 2019 GOQDs into the qRT-PCR system to improve its performance [161]. GOQDs can adsorb primers and TaqMan probes by π - π stacking and hydrogen bonding, thereby reducing the background fluorescence intensity of TaqMan probes, reducing the non-specific amplification in PCR reactions and improving the specificity of the detection. This GOQDs-based qRT-PCR can detect DNA sequences of two different lengths (106 bp and 65 bp) with a linear range of 10^4 - 10^{10} copies μL^{-1} . Subsequently, GO was further applied to qRT-PCR to establish a GO-based qRT-PCR assay to detect ovarian cancer-associated miRNAs (Fig. 7a) [162]. Our group discovered that the pre-adsorbing of the primers on the GO surface improves the efficiency of PCR amplification by increasing the efficiency of the primer template hybridization and reducing the non-specific amplification, thus increasing the sensitivity of qRT-PCR. The minimum detection limit of the assay is 10-fold lower than that of conventional qRT-PCR, and the detection of miRNAs associated with ovarian cancer confirms that

GO-based qRT-PCR assay can differentiate benign ovarian tumors from ovarian cancer (sensitivity, 0.91; specificity, 1.00).

In addition to introducing CNs alone into the qRT-PCR system, several groups have also achieved a sensitive diagnosis of diseases by constructing complexes based on CNs. Kim et al. detected the foot-and-mouth disease virus (FMDV) with high sensitivity by constructing nanocomposites of GO and AuNPs and introducing them into a qRT-PCR system [163]. The citrate in AuNPs selectively binds the ssDNA by electrostatic attraction but not the dsDNA [164,165], enabling the nanocomposite of GO and AuNPs to interact between primers and templates during DNA replication by acting like a single-stranded DNA binding protein (SSB). GO-AuNPs increased the detection limit of qRT-PCR by approximately 1000-fold and the threshold cycle (Ct) value was 4–5 cycles lower than that of the qRT-PCR with the addition of GO only. Jung and coworkers developed composite microparticles of a primer-immobilized network (cPIN) based on CNTs and used multiplex qRT-PCR to detect *Acinetobacter baumannii*, *E. coli*, *Klebsiella pneumoniae*, and *Pseudomonas aeruginosa* (Fig. 7b) [166]. One of the specific pair of primers in cPIN is adsorbed on the surface of CNTs, and the other primer is adsorbed in a prepolymer of poly(ethylene glycol)-diacrylate (PEGDA) and acrylate. The increase of temperature during qRT-PCR induces the dissociation of the primers from the surface of CNTs, and the qRT-PCR reaction occurs to achieve multiplex detection of pathogenic bacteria.

Most studies have focused only on the potential mechanisms of CNs as PCR enhancers despite the abundance of research devoted to the application of these nanomaterials in improving PCR performance, with few of these studies focusing in PCR techniques directly applied to the detection of nucleic acid biomarkers in patient specimens for clinically relevant diseases. Nonetheless, these studies also provide strong evidence that CNs have the potential to improve the performance of PCR and may be a potential platform for infectious diseases and tumors diagnosis.

5.2. Improvement of other NAAT systems

In addition to the introduction of CNs into PCR systems, several studies explored the utility of CNs in other NAATs. RCA is one of the thermostable NAATs that uses a circular template and a special DNA polymerase (e.g., Phi29) to achieve a targeted amplification [167]. Wang et al. developed a GO-based RCA technique to detect the intracellular ATP, where GO can adsorb three types of DNA (template DNA, signal DNA, and linker DNA), quenching the fluorescence signal of DNA by FRET (Fig. 7c) [168]. The specific binding of ATP to template DNA elicits the hybridization of the linker DNA with template DNA eventually triggered by RCA, quantifying ATP by the fluorescent signal generated from the hybridization of the RCA product with the signal DNA (LOD, 2×10^{-8} M). In addition, Lin et al. established a GO-based LAMP approach for the one-step detection of cyclooxygenase-2 (B) mRNA in cancer cells and serum samples [169]. LAMP technology amplifies nucleic acids in a short time (usually within 1 h) at isothermal (60–65 °C) conditions. GO in the LAMP system can greatly enhance the specificity of LAMP by reducing the non-specific hybridization and fluorescent background signals, with a detection limit of two orders of magnitude higher than that of the classical LAMP. In 2021, Choi used RPA as an isothermal DNA amplification method in combination with the enzymatic *in situ* synthetic probe (rkDNA)-GO probe system for rapid detection of SARS-CoV-2 *N* gene with high sensitivity and selectivity (LOD, 6.0 aM) [170]. The fluorescence of rkDNA was completely quenched in the presence of GO, however, when the quenched rkDNA-GO system was incorporated into the RPA amplification system of SARS-CoV-2 *N* gene, the fluorescence was significantly recovered. As regard the thermostatic NAAT based on fluorescence signal for the detection of the target, the use of CNs can result in a double-edged sword. On the one hand, the quenching effect of CNs on fluorescence can reduce the background fluorescence intensity. On the other hand, since the reaction temperature

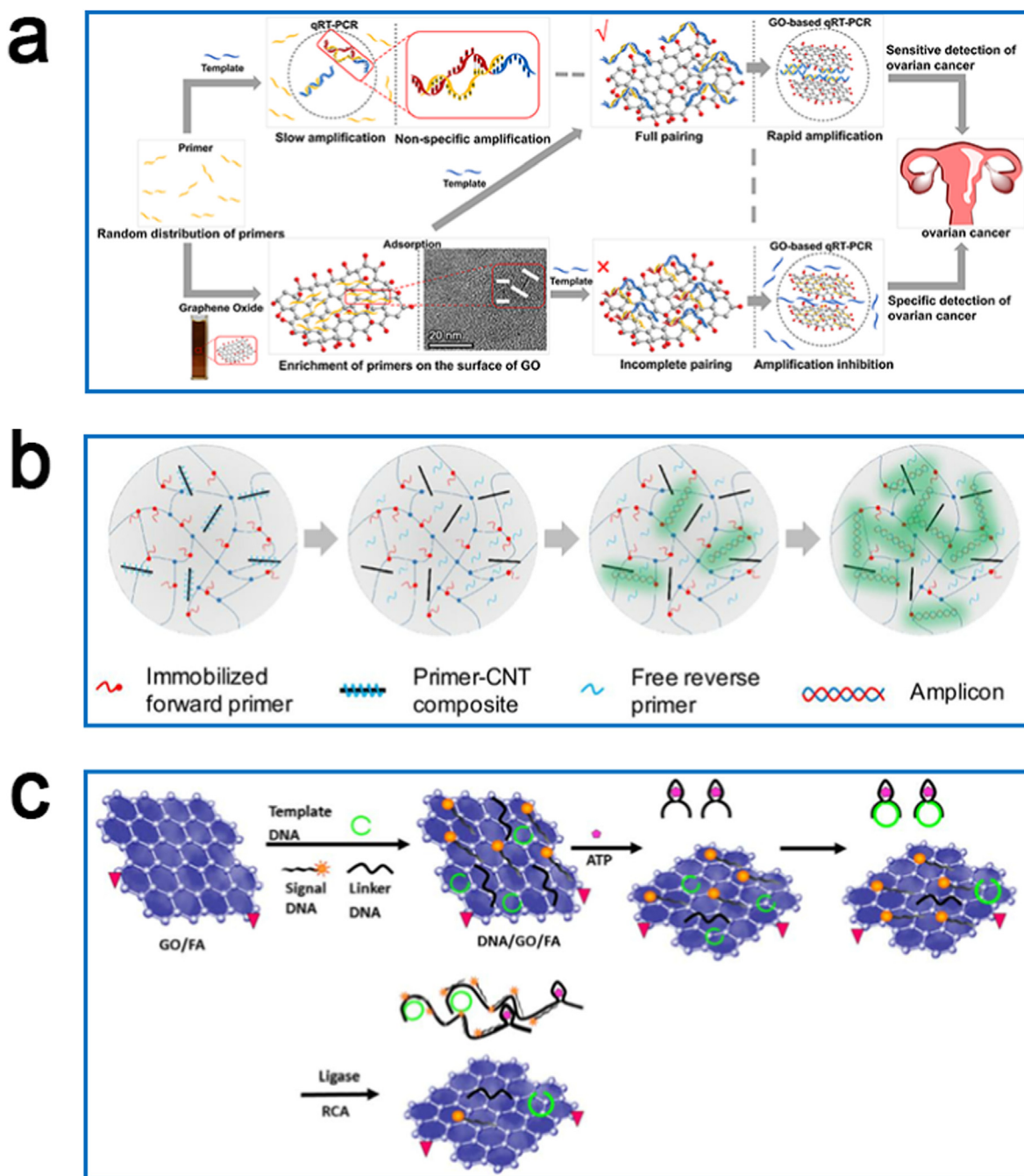


Fig. 7. Schematic view of NAAT for biomarker detection. Schematic diagrams of GO-based qRT-PCR (a), CNT-based multiplex qRT-PCR (b) and GO-based RCA (c) for biomarker detection. Reproduced with permission from Refs. [162,166,168] (Copyright 2021 and 2017, Elsevier).

of the thermostatic NAAT is often low, this interaction does not favor the recovery of the fluorescence during the reaction, thus potentially affecting the sensitivity and specificity of the assay. Despite that, the above studies confirmed the potential of CNs for NAAT applications, and the further application of these carbon nanomaterial-based NAAT in clinical practice could be potentially helpful in the early diagnosis of diseases.

6. Conclusions and Perspectives

A detailed summary and discussion of the recent advances in CNs, especially CN-based biosensors, bioimaging technologies and NAATs for the diagnosis of infectious diseases and tumors over the past five years is performed in this review. The unique optical and electrochemical

properties as well as the surface tunability of CNs make them extremely suitable for several applications. Recently, critical aspects such as emerging outbreaks of epidemic infectious diseases (e.g., SARS-CoV-2) and the requirement of an early diagnosis of difficult-to-treat diseases (e.g., tumors) encouraged the application of CNs in biomedicine. A variety of diagnostic systems have been established based on CNs functionalized biosensors, bioimaging contrast agents, and NAAT enhancers for the identification of pathogenic genes, proteases, glycans, and lesion sites.

Despite the promising application of these diagnostic technologies, several crucial points still need to be resolved before their practical application in clinical disease diagnosis. The rapid development of diagnostic technologies for emerging infectious diseases is a typical problem. As an example, the SARS-CoV-2 virus, which emerged in late

2019, has now escalated into a global pandemic. The common clinical diagnosis of viruses relies on 2 main axes: (i) direct detection of viral nucleic acids by qRT-PCR techniques; or (ii) indirect diagnosis with serological profiles specific to viral infections. These techniques have deficiencies in terms of equipment requirements, personnel training, and sensitivity. Although there has been a large amount of research aimed at designing portable sensing devices for virus diagnosis, most of the studies have focused on virus recognition with virus-specific antigen/antibody/capture nucleic acid sequences. It is well known that the design and preparation of virus-specific antigen/antibody/capture nucleic acid sequences is a time-consuming and complex procedure, which is detrimental for the prompt diagnosis of emerging infectious diseases. Therefore, the exploitation of biometric elements with simple preparation techniques is a critical challenge, offering a promising research strategy for the early diagnosis of infectious diseases and tumors.

In addition, the development of CNs-based diagnostic technologies (especially in the field of biosensing) still suffers from the following problems. First of all, the stability of the established analytical techniques is a salient issue in disease diagnosis that is essential for the potential diagnostic application of CNs. Although the current techniques are often reproducible using standard samples, the standardization of materials remains elusive. Currently established diagnostic techniques are typically stable within a few weeks to one month of a batch [171], but ensuring that a specific amount and structural properties of CNs remain the same from batch to batch is still a challenge. In general, oxygen-containing groups on the surface of CNs increase the aqueous solubility, but the oxidation process also introduces uncertainties into defecting surface areas [172]. The presence of these heterogeneities poses difficulties for the inter-batch reproducible detection of clinical biomarkers. Thus, it is essential to establish standard operating procedures (SOPs) during CNs preparation and to strictly implement them in subsequent experiments. In addition, the different suitability of clinical specimens affects the stability of the analytical techniques. Although most studies measured substances in the samples (e.g., whole blood, serum/plasma, and urine) that may interfere with the detection results [70], the specificity of the assay may be compromised in the complex real environment of the clinical samples because of the existence of numerous unknown proteins and other interfering substances. Accordingly, the current study is inadequate only for spiked clinical samples, whereas a large-scale testing of real clinical samples is of great importance to generate accurate diagnostic results. Besides, since biomarkers with similar detection principles are routinely integrated into the device used for the determination in clinical practice, the construction of integrated detection platforms for different biomarkers based on analogous detection technologies is also an area that should be investigated. The combined detection and analysis of different biomarkers is imperative for the accurate diagnosis of diseases. Although the studies on CN-based diagnostics are still in their infancy, and most of them focus on the detection of a specific biomarker, the rapid and integrated detection of multiple biomarkers is the consequent research direction in the future. Several studies focused on the combined detection of homologous biomarkers [77,173], while studies related to the construction of integrated detection platforms for biomarkers with comparable detection principles are still missing, and the integration of such platforms could become a potential promising strategy for disease diagnosis.

The toxicity of CNs is also a specific concern when applied *in vivo*, especially as contrast agents for *in vivo* bioimaging. Numerous reports demonstrated that myeloperoxidase *in vivo* is capable of producing hypochlorite to degrade CNs [174,175]. Currently, most of the studies on CNs degradation have focused on oxidized CNs owing to their favorable biocompatibility and dispersibility [176]. Nevertheless, depending on the preparation method, CNs in an aggregated state are usually difficult to be completely degraded due to the small area of binding to the enzyme [177]. Furthermore, during the preparation process, multitudes of researchers frequently encapsulate CNs with polymers in pursuit of low toxicity, which further interferes with the interaction between enzymes

and CNs [175]. Although related studies proved that CNs can be completely degraded by enzymatic catalysis *in vitro*, it still seems to be challenging to achieve complete degradation of CNs in living organisms. Accordingly, the potential long-term toxicity and degradation of CNs in organisms remains an ongoing concern.

Last but not least, the development of diagnostic technologies based on CNs is still in its infancy. According to the reported results, a cross-sectional comparison between various assays is currently not possible. On the one hand, the majority of researches on diagnostic technologies developed based on CNs are still at the stage of proof of concept or analysis of a small number of patient samples (<100 samples). The accuracy and methodological stability of these methods when applied to large clinical samples remains to be proven. On the other hand, although many researchers are currently inclined to develop POC testing devices (mainly including various sensing devices), the results of POC testing can only provide clinicians with references for further work and cannot be regarded as a direct basis for diagnosis. In terms of SARS-CoV-2 testing, the final diagnosis still depends on the combination of qRT-PCR results and CT results as diagnostic criteria. Therefore, whether the combined analysis between test results can improve the accuracy of disease diagnosis may be the direction clinicians expect to investigate. In the case of tumor detection, both the detection of tumor-associated nucleic acids by electrochemical detection techniques and NAAT, as well as the imaging of tumor sites by bioimaging techniques is possible. However, according to the current studies, it is still unknown whether the combined analysis of these test results can increase the accuracy of disease diagnosis.

In conclusion, biosensors, bioimaging technologies and NAAT based on CNs represent a new generation of promising diagnostic tools destined to gain popularity in clinical practice in the near future.

Credit author statement

Yang He: Conceptualization, Funding acquisition, Investigation, Supervision, Writing – original draft, Writing – review & editing. Chenyan Hu: Investigation, Visualization, Writing – original draft, Writing – review & editing. Zhijia Li: Investigation, Resources. Chuan Wu: Data curation. Yuanyuan Zeng: Visualization. Cheng Peng: Conceptualization, Investigation, Project administration, Supervision, Writing – original draft, Writing – review & editing.

Declaration of competing interest

The authors declare that they have no known competing financial interests or personal relationships that could have appeared to influence the work reported in this paper.

Acknowledgements

This study was financially supported by National Administration of Traditional Chinese Medicine (Grant No. ZZYCXDT-D-202209) and by the scientific research fund of Sichuan health commission (Grant No. 20PJ164).

Appendix A. Supplementary data

Supplementary data to this article can be found online at <https://doi.org/10.1016/j.mtbio.2022.100231>.

References

- [1] K. Stadler, V. Massignani, M. Eickmann, S. Becker, S. Abrignani, H.-D. Klenk, R. Rappuoli, SARS — beginning to understand a new virus, *Nat. Rev. Microbiol.* 1 (2003) 209–218, <https://doi.org/10.1038/nrmicro775>.
- [2] Z.A. Memish, S. Perlman, M.D. van Kerkhove, A. Zumla, Middle East respiratory syndrome, *Lancet* 395 (2020) 1063–1077, [https://doi.org/10.1016/S0140-6736\(19\)33221-0](https://doi.org/10.1016/S0140-6736(19)33221-0).

- [3] N. Zhu, D. Zhang, W. Wang, X. Li, B. Yang, J. Song, X. Zhao, B. Huang, W. Shi, R. Lu, P. Niu, F. Zhan, X. Ma, D. Wang, W. Xu, G. Wu, G.F. Gao, W. Tan, A novel coronavirus from patients with pneumonia in China, 2019, *N. Engl. J. Med.* 382 (2020) 727–733, <https://doi.org/10.1056/NEJMoa2001017>.
- [4] J. Payandehpeyman, N. Parvini, K. Moradi, N. Hashemian, Detection of SARS-CoV-2 using antibody–antigen interactions with graphene-based nanomechanical resonator sensors, *ACS Appl. Nano Mater.* 4 (2021) 6189–6200, <https://doi.org/10.1021/acsnm.1c00983>.
- [5] N.K. Mehra, A.K. Jain, M. Nahar, Carbon nanomaterials in oncology: an expanding horizon, *Drug Discov. Today* 23 (2018) 1016–1025, <https://doi.org/10.1016/j.drudis.2017.09.013>.
- [6] X.P. He, H. Tian, Photoluminescence architectures for disease diagnosis: from graphene to thin-layer transition metal dichalcogenides and oxides, *Small* 12 (2016) 144–160, <https://doi.org/10.1002/sml.201502516>.
- [7] A.A.S. Gill, S. Singh, N. Thapliyal, R. Karpoomath, Nanomaterial-based optical and electrochemical techniques for detection of methicillin-resistant *Staphylococcus aureus*: a review, *Microchim. Acta* 186 (2019) 114, <https://doi.org/10.1007/s00604-018-3186-7>.
- [8] Y.V. Kaneti, N.L. Wulan Septiani, I. Saptiama, X. Jiang, B. Yulianto, M.J.A. Shiddiky, N. Fukumitsu, Y.-M. Kang, D. Golberg, Y. Yamauchi, Self-sacrificial templated synthesis of a three-dimensional hierarchical macroporous honeycomb-like ZnO/ZnCo₂O₄ hybrid for carbon monoxide sensing, *J. Mater. Chem.* 7 (2019) 3415–3425, <https://doi.org/10.1039/C8TA11380G>.
- [9] J. Wen, Y. Xu, H. Li, A. Lu, S. Sun, Recent applications of carbon nanomaterials in fluorescence biosensing and bioimaging, *Chem. Commun.* 51 (2015) 11346–11358, <https://doi.org/10.1039/c5cc02887f>.
- [10] N.L. Teradal, R. Jelinek, Carbon nanomaterials in biological studies and biomedicine, *Adv. Healthc. Mater.* 6 (2017) 1700574, <https://doi.org/10.1002/adhm.201700574>.
- [11] K. Huth, M. Glaeske, K. Achazi, G. Gordeev, S. Kumar, R. Arenal, S.K. Sharma, M. Adeli, A. Setaro, S. Reich, R. Haag, Fluorescent polymer–single-walled carbon nanotube complexes with charged and noncharged dendronized perylene bisimides for bioimaging studies, *Small* 14 (2018) 1800796, <https://doi.org/10.1002/sml.201800796>.
- [12] R. Gonzalez-Rodriguez, E. Campbell, A. Naumov, Multifunctional graphene oxide/iron oxide nanoparticles for magnetic targeted drug delivery dual magnetic resonance/fluorescence imaging and cancer sensing, *PLoS One* 14 (2019), e0217072, <https://doi.org/10.1371/journal.pone.0217072>.
- [13] W. Xu, J. Chen, S. Sun, Z. Tang, K. Jiang, L. Song, Y. Wang, C. Liu, H. Lin, Fluorescent and photoacoustic bifunctional probe for the detection of ascorbic acid in biological fluids, living cells and: *in vivo*, *Nanoscale* 10 (2018) 17834–17841, <https://doi.org/10.1039/c8nr03435d>.
- [14] L. Lei, H. Ma, M. Yang, Y. Qin, Y. Ma, T. Wang, Y. Yang, Z. Lei, D. Lu, X. Guan, Fluorophore-functionalized graphene oxide with application in cell imaging, *New J. Chem.* 41 (2017) 12375–12379, <https://doi.org/10.1039/c7nj02416a>.
- [15] M. Sebaa, T.Y. Nguyen, R.K. Paul, A. Mulchandani, H. Liu, Graphene and carbon nanotube-graphene hybrid nanomaterials for human embryonic stem cell culture, *Mater. Lett.* 92 (2013) 122–125, <https://doi.org/10.1016/j.matlet.2012.10.035>.
- [16] X. Yan, W. Yang, Z. Shao, S. Yang, X. Liu, Graphene/single-walled carbon nanotube hybrids promoting osteogenic differentiation of mesenchymal stem cells by activating p38 signaling pathway, *Int. J. Nanomed.* 11 (2016) 5473–5484, <https://doi.org/10.2147/IJN.S115468>.
- [17] S. Kang, J. Lee, S. Ryu, Y. Kwon, K.H. Kim, D.H. Jeong, S.R. Paik, B.S. Kim, Gold nanoparticle/graphene oxide hybrid sheets attached on mesenchymal stem cells for effective photothermal cancer therapy, *Chem. Mater.* 29 (2017) 3461–3476, <https://doi.org/10.1021/acs.chemmater.6b05164>.
- [18] S. Selvarajan, A. Suganthi, M. Rajarajan, A simple sonochemical approach to fabricate a urea biosensor based on zinc phthalocyanine/graphene oxide/urease bioelectrode, *Ultrason. Sonochem.* 42 (2018) 183–192, <https://doi.org/10.1016/j.ultrsonch.2017.11.030>.
- [19] J. Pilas, T. Selmer, M. Keusgen, M.J. Schöning, Screen-printed carbon electrodes modified with graphene oxide for the design of a reagent-free NAD⁺-dependent biosensor array, *Anal. Chem.* 91 (2019) 15293–15299, <https://doi.org/10.1021/acs.analchem.9b04481>.
- [20] L. Zhu, X. Feng, S. Yang, J. Wang, Y. Pan, J. Ding, C. Li, X. Yin, Y. Yu, Colorimetric detection of immunomagnetically captured rare number CTCs using mDNA-wrapped single-walled carbon nanotubes, *Biosens. Bioelectron.* 172 (2021) 112780, <https://doi.org/10.1016/j.bios.2020.112780>.
- [21] M. Mohajeri, B. Behnam, A. Sahebkar, Biomedical applications of carbon nanomaterials: drug and gene delivery potentials, *J. Cell. Physiol.* 234 (2018) 298–319, <https://doi.org/10.1002/jcp.26899>.
- [22] S. Tajik, Z. Dourandish, K. Zhang, H. Beitollahi, Q. van Le, H.W. Jang, M. Shokouhimehr, Carbon and graphene quantum dots: a review on syntheses, characterization, biological and sensing applications for neurotransmitter determination, *RSC Adv.* 10 (2020) 15406–15429, <https://doi.org/10.1039/D0RA00799D>.
- [23] J.C. Coyuco, Y. Liu, B.J. Tan, G.N.C. Chiu, Functionalized carbon nanomaterials: exploring the interactions with Caco-2 cells for potential oral drug delivery, *Int. J. Nanomed.* 6 (2011) 2253–2263, <https://doi.org/10.2147/IJN.S23962>.
- [24] V. Biju, Chemical modifications and bioconjugate reactions of nanomaterials for sensing, imaging, drug delivery and therapy, *Chem. Soc. Rev.* 43 (2014) 744–764, <https://doi.org/10.1039/c3cs60273g>.
- [25] D. Chen, C.A. Dougherty, K. Zhu, H. Hong, Theranostic applications of carbon nanomaterials in cancer: focus on imaging and cargo delivery, *J. Contr. Release* 210 (2015) 230–245, <https://doi.org/10.1016/j.jconrel.2015.04.021>.
- [26] E.S. Shibu, M. Hamada, N. Murase, V. Biju, Nanomaterials formulations for photothermal and photodynamic therapy of cancer, *J. Photochem. Photobiol. C Photochem. Rev.* 15 (2013) 53–72, <https://doi.org/10.1016/j.jphotochemrev.2012.09.004>.
- [27] B. Jiang, B. Zhou, Z. Lin, H. Liang, X. Shen, Recent advances in carbon nanomaterials for cancer phototherapy, *Chem. Eur. J.* 25 (2019) 3993–4004, <https://doi.org/10.1002/chem.201804383>.
- [28] H. Taheri, M.A. Unal, M. Sevim, C. Gurcan, O. Ekim, A. Ceylan, Z. Syrgiannis, K.C. Christoforidis, S. Bosi, O. Ozgenç, M.J. Gómez, M. Turktas Erken, Ç. Soydal, Z. Eroglu, C.V. Bitirim, U. Cagin, F. Ari, A. Ozen, O. Kuçuk, L.G. Delogu, M. Prato, Ö. Metin, A. Yilmazer, Photocatalytically active graphitic carbon nitride as an effective and safe 2D material for *in vitro* and *in vivo* photodynamic therapy, *Small* 16 (2020) 1904619, <https://doi.org/10.1002/sml.201904619>.
- [29] K.D. Patel, R.K. Singh, H.W. Kim, Carbon-based nanomaterials as an emerging platform for theranostics, *Mater. Horizons* 6 (2019) 434–469, <https://doi.org/10.1039/c8mh00966j>.
- [30] H.S. Hwang, J.W. Jeong, Y.A. Kim, M. Chang, Carbon nanomaterials as versatile platforms for biosensing applications, *Micromachines* 11 (2020) 814, <https://doi.org/10.3390/M11090814>.
- [31] N. Yadav, M. Tyagi, S. Wadhwa, A. Mathur, J. Narang, Few biomedical applications of carbon nanotubes, *Methods Enzymol.* 630 (2020) 347–363, <https://doi.org/10.1016/bs.mie.2019.11.005>.
- [32] M. Roldo, D.G. Fatouros, Biomedical applications of carbon nanotubes, *Annu. Reports Prog. Chem. - Sect. C* 109 (2013) 10–35, <https://doi.org/10.1039/c3pc90010j>.
- [33] G. Chen, D.N. Futaba, S. Sakurai, M. Yumura, K. Hata, Interplay of wall number and diameter on the electrical conductivity of carbon nanotube thin films, *Carbon* 67 (2014) 318–325, <https://doi.org/10.1016/j.carbon.2013.10.001>.
- [34] R.R. Pandey, C.C. Chusuei, Carbon nanotubes, graphene, and carbon dots as electrochemical biosensing composites, *Molecules* 26 (2021) 6674, <https://doi.org/10.3390/molecules26216674>.
- [35] Y. Luo, Y. Wang, H. Yan, Y. Wu, C. Zhu, D. Du, Y. Lin, SWCNTs@GQDs composites as nanocarriers for enzyme-free dual-signal amplification electrochemical immunoassay of cancer biomarker, *Anal. Chim. Acta* 1042 (2018) 44–51, <https://doi.org/10.1016/j.aca.2018.08.023>.
- [36] A. Sabahi, R. Salahandish, A. Ghaffarinejad, E. Omidinia, Electrochemical nanosensor for highly sensitive detection of miR-21 biomarker based on SWCNT-grafted dendritic Au nanostructure for early detection of prostate cancer, *Talanta* 209 (2020) 120595, <https://doi.org/10.1016/j.talanta.2019.120595>.
- [37] N. do Quyen Chau, C. Ménard-Moyon, K. Kostarelos, A. Bianco, Multifunctional carbon nanomaterial hybrids for magnetic manipulation and targeting, *Biochem. Biophys. Res. Commun.* 468 (2015) 454–462, <https://doi.org/10.1016/j.bbrc.2015.06.131>.
- [38] R.K. Singh, K.D. Patel, J.J. Kim, T.H. Kim, J.H. Kim, U.S. Shin, E.J. Lee, J.C. Knowles, H.W. Kim, Multifunctional hybrid nanocarrier: magnetic CNTs enshathed with mesoporous silica for drug delivery and imaging system, *ACS Appl. Mater. Interfaces* 6 (2014) 2201–2208, <https://doi.org/10.1021/am4056936>.
- [39] H. Ehtesabi, Application of carbon nanomaterials in human virus detection, *J. Sci. Adv. Mater. Devices* 5 (2020) 436–450, <https://doi.org/10.1016/j.jsamd.2020.09.005>.
- [40] R. Zhang, S. Wang, X. Huang, Y. Yang, H. Fan, F. Yang, J. Li, X. Dong, S. Feng, P. Anbu, S.C.B. Gopinath, T. Xin, Gold-nanourchin seeded single-walled carbon nanotube on voltammetry sensor for diagnosing neurodegenerative Parkinson's disease, *Anal. Chim. Acta* 1094 (2020) 142–150, <https://doi.org/10.1016/j.aca.2019.10.012>.
- [41] Y. Ishibashi, S. Oura, K. Umemura, Adsorption of DNA binding proteins to functionalized carbon nanotube surfaces with and without DNA wrapping, *Eur. Biophys. J.* 46 (2017) 541–547, <https://doi.org/10.1007/s00249-017-1200-3>.
- [42] M.K. Masud, J. Na, M. Younus, M.S.A. Hossain, Y. Bando, M.J.A. Shiddiky, Y. Yamauchi, Superparamagnetic nanoarchitectures for disease-specific biomarker detection, *Chem. Soc. Rev.* 48 (2019) 5717–5751, <https://doi.org/10.1039/C9CS00174C>.
- [43] Z. Wan, M. Umer, M. Lobino, D. Thiel, N.-T. Nguyen, A. Trinchi, M.J.A. Shiddiky, Y. Gao, Q. Li, Laser induced self-N-doped porous graphene as an electrochemical biosensor for femtomolar miRNA detection, *Carbon* 163 (2020) 385–394, <https://doi.org/10.1016/j.carbon.2020.03.043>.
- [44] G. Hong, S. Diao, A.L. Antaris, H. Dai, Carbon nanomaterials for biological imaging and nanomedicinal therapy, *Chem. Rev.* 115 (2015) 10816–10906, <https://doi.org/10.1021/acs.chemrev.5b00008>.
- [45] Y. Huang, M. Shi, L. Zhao, S. Zhao, K. Hu, Z.F. Chen, J. Chen, H. Liang, Carbon nanotube signal amplification for ultrasensitive fluorescence polarization detection of DNA methyltransferase activity and inhibition, *Biosens. Bioelectron.* 54 (2014) 285–291, <https://doi.org/10.1016/j.bios.2013.10.065>.
- [46] M. Zhang, W. Wang, Y. Cui, X. Chu, B. Sun, N. Zhou, J. Shen, Magneto-fluorescent Fe₃O₄/carbon quantum dots coated single-walled carbon nanotubes as dual-modal targeted imaging and chemo/photodynamic/photothermal triple-modal therapeutic agents, *Chem. Eng. J.* 338 (2018) 526–538, <https://doi.org/10.1016/j.cej.2018.01.081>.
- [47] D. Cui, F. Tian, Y. Kong, I. Titushkin, H. Gao, Effects of single-walled carbon nanotubes on the polymerase chain reaction, *Nanotechnology* 15 (2004) 154–157, <https://doi.org/10.1088/0957-4484/15/1/030>.
- [48] Z. Zhang, X. Xiang, Y. Hu, Y. Deng, L. Li, W. Zhao, T. Wu, A sensitive biomolecules detection device with catalytic hairpin assembly and cationic conjugated polymer-assisted dual signal amplification strategy, *Talanta* 223 (2021) 121716, <https://doi.org/10.1016/j.talanta.2020.121716>.

- [49] Z. Liu, J.T. Robinson, X. Sun, H. Dai, PEGylated nanographene oxide for delivery of water-insoluble cancer drugs, *J. Am. Chem. Soc.* 130 (2008) 10876–10877, <https://doi.org/10.1021/ja803688x>.
- [50] X. Wu, Y. Chuang, A. Contino, B. Sorée, S. Brems, Z. Tokei, M. Heyns, C. Huyghebaert, I. Asselberghs, Boosting carrier mobility of synthetic few layer graphene on SiO₂ by interlayer rotation and decoupling, *Adv. Mater. Interfac.* 5 (2018) 1800454, <https://doi.org/10.1002/admi.201800454>.
- [51] S. Li, S. Huang, Y. Ke, H. Chen, J. Dang, C. Huang, W. Liu, D. Cui, J. Wang, X. Zhi, X. Ding, A HIPAD integrated with rGO/MWCNTs nano-circuit heater for visual point-of-care testing of SARS-CoV-2, *Adv. Funct. Mater.* 31 (2021) 2100801, <https://doi.org/10.1002/adfm.202100801>.
- [52] Y. Zhao, K. Li, Z. He, Y. Zhang, Y. Zhao, H. Zhang, Z. Miao, Investigation on fluorescence quenching mechanism of perylene diimide dyes by graphene oxide, *Molecules* 21 (2016) 1642, <https://doi.org/10.3390/molecules21121642>.
- [53] F. Mouhat, F.X. Coudert, M.L. Bocquet, Structure and chemistry of graphene oxide in liquid water from first principles, *Nat. Commun.* 11 (2020) 1566, <https://doi.org/10.1038/s41467-020-15381-y>.
- [54] D. Maiti, X. Tong, X. Mou, K. Yang, Carbon-based nanomaterials for biomedical applications: a recent study, *Front. Pharmacol.* 9 (2019) 1401, <https://doi.org/10.3389/fphar.2018.01401>.
- [55] Z. Dehghani, M. Mohammadnejad, M. Hosseini, B. bakhshi, A.H. Rezayan, Whole cell FRET immunosensor based on graphene oxide and graphene dot for *Campylobacter jejuni* detection, *Food Chem.* 309 (2020) 125690, <https://doi.org/10.1016/j.foodchem.2019.125690>.
- [56] G. Fan, R. Wan, B. Zhang, S. Deng, M. Peng, W. Xue, L. Xu, X. Qin, Y. Wu, The Distribution and imaging of ^{99m}Tc-nGO-PEG-FA in human patu8988 tumor-bearing nude mice, *Cancer Biother. Radiopharm* 33 (2018) 445–459, <https://doi.org/10.1089/cbr.2017.2395>.
- [57] Y. Toumia, B. Cerroni, P. Trochet, S. Lacerenza, L. Oddo, F. Domenici, G. Paradossi, Performances of a pristine graphene–microbubble hybrid construct as dual imaging contrast agent and assessment of its biodistribution by photoacoustic imaging, *Part. Part. Syst. Char.* 35 (2018) 1800066, <https://doi.org/10.1002/ppsc.201800066>.
- [58] Z. yue Wang, P. Li, L. Cui, J.G. Qiu, B.H. Jiang, C. yang Zhang, Integration of nanomaterials with nucleic acid amplification approaches for biosensing, *TrAC Trends Anal. Chem. (Reference Ed.)* 129 (2020) 115959, <https://doi.org/10.1016/j.trac.2020.115959>.
- [59] S. Li, Z. Wang, Y. Wang, M. Song, G. Lu, N. Dang, H. Yin, Y. Qu, Y. Deng, Effects of graphene oxide on PCR amplification for microbial community survey, *BMC Microbiol.* 20 (2020) 278, <https://doi.org/10.1186/s12866-020-01965-7>.
- [60] J. Li, D. Wu, Y. Yu, T. Li, K. Li, M.-M. Xiao, Y. Li, Z.-Y. Zhang, G.-J. Zhang, Rapid and unamplified identification of COVID-19 with morpholino-modified graphene field-effect transistor nanosensor, *Biosens. Bioelectron.* 183 (2021) 113206, <https://doi.org/10.1016/j.bios.2021.113206>.
- [61] I. Novodchuk, M. Kayaharman, I.R. Ausri, R. Karimi, X.S. Tang, I.A. Goldthorpe, E. Abdel-Rahman, J. Sanderson, M. Bajcsy, M. Yavuz, An ultrasensitive heart-failure BNP biosensor using B/N co-doped graphene oxide gel FET, *Biosens. Bioelectron.* 180 (2021) 113114, <https://doi.org/10.1016/j.bios.2021.113114>.
- [62] X. Xu, R. Ray, Y. Gu, H.J. Ploehn, L. Gearheart, K. Raker, W.A. Scrivens, Electrophoretic analysis and purification of fluorescent single-walled carbon nanotube fragments, *J. Am. Chem. Soc.* 126 (2004) 12736–12737, <https://doi.org/10.1021/ja040082h>.
- [63] C. Ji, Y. Zhou, R.M. Leblanc, Z. Peng, Recent developments of carbon dots in biosensing: a review, *ACS Sens.* 5 (2020) 2724–2741, <https://doi.org/10.1021/acssens.0c01556>.
- [64] D. Li, P. Jing, L. Sun, Y. An, X. Shan, X. Lu, D. Zhou, D. Han, D. Shen, Y. Zhai, S. Qu, R. Zboril, A.L. Rogach, Near-infrared excitation/emission and multiphoton-induced fluorescence of carbon dots, *Adv. Mater.* 30 (2018) 1705913, <https://doi.org/10.1002/adma.201705913>.
- [65] Y. Su, X. Zhou, Y. Long, W. Li, Immobilization of horseradish peroxidase on amino-functionalized carbon dots for the sensitive detection of hydrogen peroxide, *Microchim. Acta* 185 (2018) 114, <https://doi.org/10.1007/s00604-017-2629-x>.
- [66] Z. Gao, Y. Nakanishi, S. Noda, H. Omachi, H. Shinohara, H. Kimura, Y. Nagasaki, Development of Gd₃N@C₈₀ encapsulated redox nanoparticles for high-performance magnetic resonance imaging, *J. Biomater. Sci. Polym. Ed.* 28 (2017) 1036–1050, <https://doi.org/10.1080/09205063.2017.1288774>.
- [67] R. Kour, S. Arya, S.-J. Young, V. Gupta, P. Bandhoria, A. Khosla, Review—recent advances in carbon nanomaterials as electrochemical biosensors, *J. Electrochem. Soc.* 167 (2020), 037555, <https://doi.org/10.1149/1945-7111/ab6bc4>.
- [68] K.-D. Seo, M.M. Hossain, N.G. Gurudatt, C.S. Choi, M.J.A. Shiddiky, D.-S. Park, Y.-B. Shim, Microfluidic neurotransmitter sensor in blood plasma with mediator-immobilized conducting polymer/N, S-doped porous carbon composite, *Sensor. Actuator. B Chem.* 313 (2020) 128017, <https://doi.org/10.1016/j.snb.2020.128017>.
- [69] Z. Wang, Z. Dai, Carbon nanomaterial-based electrochemical biosensors: an overview, *Nanoscale* 7 (2015) 6420–6431, <https://doi.org/10.1039/c5nr00585j>.
- [70] Y. Chen, S. Guo, M. Zhao, P. Zhang, Z. Xin, J. Tao, L. Bai, Amperometric DNA biosensor for *Mycobacterium tuberculosis* detection using flower-like carbon nanotubes-polyaniline nanohybrid and enzyme-assisted signal amplification strategy, *Biosens. Bioelectron.* 119 (2018) 215–220, <https://doi.org/10.1016/j.bios.2018.08.023>.
- [71] H. Zhao, F. Liu, W. Xie, T.C. Zhou, J. OuYang, L. Jin, H. Li, C.Y. Zhao, L. Zhang, J. Wei, Y.P. Zhang, C.P. Li, Ultrasensitive supersandwich-type electrochemical sensor for SARS-CoV-2 from the infected COVID-19 patients using a smartphone, *Sensor. Actuator. B Chem.* 327 (2021) 128899, <https://doi.org/10.1016/j.snb.2020.128899>.
- [72] L. Bai, Y. Chen, X. Liu, J. Zhou, J. Cao, L. Hou, S. Guo, Ultrasensitive electrochemical detection of *Mycobacterium tuberculosis* IS6110 fragment using gold nanoparticles decorated fullerene nanoparticles/nitrogen-doped graphene nanosheet as signal tags, *Anal. Chim. Acta* 1080 (2019) 75–83, <https://doi.org/10.1016/j.aca.2019.06.043>.
- [73] J. Zuo, Y. Yuan, M. Zhao, J. Wang, Y. Chen, Q. Zhu, L. Bai, An efficient electrochemical assay for miR-3675-3p in human serum based on the nanohybrid of functionalized fullerene and metal-organic framework, *Anal. Chim. Acta* 1140 (2020) 78–88, <https://doi.org/10.1016/j.aca.2020.10.017>.
- [74] Y. Zheng, X. Wang, S. He, Z. Gao, Y. Di, K. Lu, K. Li, J. Wang, Aptamer-DNA concatamer-quantum dots based electrochemical biosensing strategy for green and ultrasensitive detection of tumor cells via mercury-free anodic stripping voltammetry, *Biosens. Bioelectron.* 126 (2019) 261–268, <https://doi.org/10.1016/j.bios.2018.09.076>.
- [75] H.R. Jamei, B. Rezaei, A.A. Ensafi, Ultra-sensitive and selective electrochemical biosensor with aptamer recognition surface based on polymer quantum dots and C₆₀/MWCNTs-polyethyleneimine nanocomposites for analysis of thrombin protein, *Bioelectrochemistry* 138 (2021) 107701, <https://doi.org/10.1016/j.bioelect.2020.107701>.
- [76] H.A. Hussein, A. Kandeil, M. Gomaa, R. Mohamed El Nashar, I.M. El-Sherbiny, R.Y.A. Hassan, SARS-CoV-2-impedimetric biosensor: virus-imprinted chips for early and rapid diagnosis, *ACS Sens.* 6 (2021) 4098–4107, <https://doi.org/10.1021/acssensors.1c01614>.
- [77] R.M. Torrente-Rodríguez, H. Lukas, J. Tu, J. Min, Y. Yang, C. Xu, H.B. Rossiter, W. Gao, SARS-CoV-2 RapidPlex, A graphene-based multiplexed telemedicine platform for rapid and low-cost COVID-19 diagnosis and monitoring, *Matter* 3 (2020), <https://doi.org/10.1016/j.matt.2020.09.027>, 1981–1998.
- [78] C. Pothipor, J. Jakmunee, S. Bamrungsap, K. Ounnunkad, An electrochemical biosensor for simultaneous detection of breast cancer clinically related microRNAs based on a gold nanoparticles/graphene quantum dots/graphene oxide film, *Analyst* 146 (2021) 4000–4009, <https://doi.org/10.1039/d1an00436k>.
- [79] S.H. Jafari, Z. Saadatpour, A. Salaminejad, F. Momeni, M. Mokhtari, J.S. Nahand, M. Rahmati, H. Mirzaei, M. Kianmehr, Breast cancer diagnosis: imaging techniques and biochemical markers, *J. Cell. Physiol.* 233 (2018) 5200–5213, <https://doi.org/10.1002/jcp.26379>.
- [80] M.T. Hwang, I. Park, M. Heiranian, A. Taqieeddin, S. You, V. Faramarzi, A.A. Pak, A.M. van der Zande, N.R. Aluru, R. Bashir, Ultrasensitive detection of dopamine, IL-6 and SARS-CoV-2 proteins on crumpled graphene FET biosensor, *Adv. Mater. Technol.* 6 (2021) 1–9, <https://doi.org/10.1002/admt.202100712>.
- [81] Y. Zhang, Q. Wan, N. Yang, Recent advances of porous graphene: synthesis, functionalization, and electrochemical applications, *Small* 15 (2019) 1903780, <https://doi.org/10.1002/sml.201903780>.
- [82] W. Shao, M.R. Shurin, S.E. Wheeler, X. He, A. Star, Rapid detection of SARS-CoV-2 antigens using high-purity semiconducting single-walled carbon nanotube-based field-effect transistors, *ACS Appl. Mater. Interfaces* 13 (2021) 10321–10327, <https://doi.org/10.1021/acsaami.0c22589>.
- [83] G. Seo, G. Lee, M.J. Kim, S.H. Baek, M. Choi, K.B. Ku, C.S. Lee, S. Jun, D. Park, H.G. Kim, S.J. Kim, J.O. Lee, B.T. Kim, E.C. Park, S. il Kim, Rapid detection of COVID-19 causative virus (SARS-CoV-2) in human nasopharyngeal swab specimens using field-effect transistor-based biosensor, *ACS Nano* 14 (2020) 5135–5142, <https://doi.org/10.1021/acsnano.0c02823>.
- [84] D. Wu, Y. Yu, D. Jin, M.-M. Xiao, Z.-Y. Zhang, G.-J. Zhang, Dual-aptamer modified graphene field-effect transistor nanosensor for label-free and specific detection of hepatocellular carcinoma-derived microvesicles, *Anal. Chem.* 92 (2020) 4006–4015, <https://doi.org/10.1021/acs.analchem.9b05531>.
- [85] Z. Hao, Y. Luo, C. Huang, Z. Wang, G. Song, Y. Pan, X. Zhao, S. Liu, An intelligent graphene-based biosensing device for cytokine storm syndrome biomarkers detection in human biofluids, *Small* 17 (2021) 1–11, <https://doi.org/10.1002/sml.202101508>.
- [86] Y. Li, Y. Zhu, C. Wang, M. He, Q. Lin, Selective detection of water pollutants using a differential aptamer-based graphene biosensor, *Biosens. Bioelectron.* 126 (2019) 59–67, <https://doi.org/10.1016/j.bios.2018.10.047>.
- [87] G. Ke, D. Su, Y. Li, Y. Zhao, H. Wang, W. Liu, M. Li, Z. Yang, F. Xiao, Y. Yuan, F. Huang, F. Mo, P. Wang, X. Guo, An accurate, high-speed, portable bifunctional electrical detector for COVID-19, *Sci. China Mater.* 64 (2021) 739–747, <https://doi.org/10.1007/s40843-020-1577-y>.
- [88] W.W. Zhao, M. Xiong, X.R. Li, J.J. Xu, H.Y. Chen, Photoelectrochemical bioanalysis: a mini review, *Electrochem. Commun.* 38 (2014) 40–43, <https://doi.org/10.1016/j.elecom.2013.10.035>.
- [89] H. Xue, K. Chen, Q. Zhou, D. Pan, Y. Zhang, Y. Shen, Antimony selenide/graphene oxide composite for sensitive photoelectrochemical detection of DNA methyltransferase activity, *J. Mater. Chem. B* 7 (2019) 6789–6795, <https://doi.org/10.1039/c9tb01541h>.
- [90] L. Meng, K. Xiao, X. Zhang, C. Du, J. Chen, A novel signal-off photoelectrochemical biosensor for M.SssI MTase activity assay based on GQDs@ZIF-8 polyhedra as signal quencher, *Biosens. Bioelectron.* 150 (2020) 111861, <https://doi.org/10.1016/j.bios.2019.111861>.
- [91] M. Amouzadeh Tabrizi, L. Nazari, P. Acedo, A photo-electrochemical aptasensor for the determination of severe acute respiratory syndrome coronavirus 2 receptor-binding domain by using graphitic carbon nitride-cadmium sulfide quantum dots nanocomposite, *Sensor. Actuator. B Chem.* 345 (2021) 130377, <https://doi.org/10.1016/j.snb.2021.130377>.
- [92] M.J. Li, Y.N. Zheng, W. bin Liang, R. Yuan, Y.Q. Chai, Using p-type PbS quantum dots to quench photocurrent of fullerene-Au NP@MoS₂ composite structure for

- ultrasensitive photoelectrochemical detection of ATP, *ACS Appl. Mater. Interfaces* 9 (2017) 42111–42120, <https://doi.org/10.1021/acsami.7b13894>.
- [93] H. Wang, M. Li, Y. Zheng, T. Hu, Y. Chai, R. Yuan, An ultrasensitive photoelectrochemical biosensor based on [Ru(dcbpy)₂dppz]²⁺/Rose Bengal dyes co-sensitized fullerene for DNA detection, *Biosens. Bioelectron.* 120 (2018) 71–76, <https://doi.org/10.1016/j.bios.2018.08.035>.
- [94] D. Long, M. Li, H. Wang, H. Wang, Y. Chai, R. Yuan, A photoelectrochemical biosensor based on fullerene with methylene blue as a sensitizer for ultrasensitive DNA detection, *Biosens. Bioelectron.* 142 (2019) 111579, <https://doi.org/10.1016/j.bios.2019.111579>.
- [95] H.H. Wang, M.J. Li, H.J. Wang, Y.Q. Chai, R. Yuan, p-n-sensitized heterostructure Co₃O₄/Fullerene with highly efficient photoelectrochemical performance for ultrasensitive DNA detection, *ACS Appl. Mater. Interfaces* 11 (2019) 23765–23772, <https://doi.org/10.1021/acsami.9b05923>.
- [96] H.H. Wang, M.J. Li, Y.P. Tu, H.J. Wang, Y.Q. Chai, Z.H. Li, R. Yuan, Fullerene as a photoelectrochemical nanoprobe for discrimination and ultrasensitive detection of amplification-free single-stranded DNA, *Biosens. Bioelectron.* 173 (2021) 112802, <https://doi.org/10.1016/j.bios.2020.112802>.
- [97] D. Wang, Y. Liang, Y. Su, Q. Shang, C. Zhang, Sensitivity enhancement of cloth-based closed bipolar electrochemiluminescence glucose sensor via electrode decoration with chitosan/multi-walled carbon nanotubes/graphene quantum dots-gold nanoparticles, *Biosens. Bioelectron.* 130 (2019) 55–64, <https://doi.org/10.1016/j.bios.2019.01.027>.
- [98] D. Bahari, B. Babamiri, A. Salimi, R. Hallaj, S.M. Amininasab, A self-enhanced ECL-RET immunosensor for the detection of CA19-9 antigen based on Ru(bpy)₂(phen-NH₂)²⁺. Amine-rich nitrogen-doped carbon nanodots as probe and graphene oxide grafted hyperbranched aromatic polyamide as platform, *Anal. Chim. Acta* 1132 (2020) 55–65, <https://doi.org/10.1016/j.aca.2020.07.023>.
- [99] Y. Wang, H. Sha, H. Ke, X. Xiong, N. Jia, A sandwich-type electrochemiluminescence aptasensor for insulin detection based on the nano-C₆₀/BSA@luminoil nanocomposite and ferrocene derivative, *Electrochim. Acta* 290 (2018) 90–97, <https://doi.org/10.1016/j.electacta.2018.08.080>.
- [100] C. Yang, Q. Guo, Y. Lu, B. Zhang, G. Nie, Ultrasensitive “signal-on” electrochemiluminescence immunosensor for prostate-specific antigen detection based on novel nanoprobe and poly(indole-6-carboxylic acid)/flower-like Au nanocomposite, *Sensor. Actuator. B Chem.* 303 (2020) 127246, <https://doi.org/10.1016/j.snb.2019.127246>.
- [101] D. Qin, X. Jiang, G. Mo, X. Zheng, B. Deng, Electrochemiluminescence immunoassay of human chorionic gonadotropin using silver carbon quantum dots and functionalized polymer nanospheres, *Microchim. Acta* 187 (2020) 482, <https://doi.org/10.1007/s00604-020-04450-0>.
- [102] Y. Iizumi, T. Okazaki, Y. Ikehara, M. Ogura, S. Fukata, M. Yudasaka, Immunoassay with single-walled carbon nanotubes as near-infrared fluorescent labels, *ACS Appl. Mater. Interfaces* 5 (2013) 7665–7670, <https://doi.org/10.1021/am401702q>.
- [103] R. Chinnappan, A.A. Rahamn, R. AlZabn, S. Kamath, A.L. Lopata, K.M. Abu-Salah, M. Zourab, Aptameric biosensor for the sensitive detection of major shrimp allergen, tropomyosin, *Food Chem.* 314 (2020) 126113, <https://doi.org/10.1016/j.foodchem.2019.126133>.
- [104] Y. Xia, M. Liu, L. Wang, A. Yan, W. He, M. Chen, J. Lan, J. Xu, L. Guan, J. Chen, A visible and colorimetric aptasensor based on DNA-capped single-walled carbon nanotubes for detection of exosomes, *Biosens. Bioelectron.* 92 (2017) 8–15, <https://doi.org/10.1016/j.bios.2017.01.063>.
- [105] X. Li, X.Y. Yang, J.Q. Sha, T. Han, C.J. Du, Y.J. Sun, Y.Q. Lan, POMOF/SWNT nanocomposites with prominent peroxidase-mimicking activity for L-Cysteine “on-off switch” colorimetric biosensing, *ACS Appl. Mater. Interfaces* 11 (2019) 16896–16904, <https://doi.org/10.1021/acsami.9b00872>.
- [106] Q. Wang, H. Pang, Y. Dong, Y. Chi, F. Fu, Colorimetric determination of glutathione by using a nanohybrid composed of manganese dioxide and carbon dots, *Microchim. Acta* 185 (2018) 291, <https://doi.org/10.1007/s00604-018-2830-6>.
- [107] Y. Bai, H. Li, J. Xu, Y. Huang, X. Zhang, J. Weng, Z. Li, L. Sun, Ultrasensitive colorimetric biosensor for BRCA1 mutation based on multiple signal amplification strategy, *Biosens. Bioelectron.* 166 (2020) 112424, <https://doi.org/10.1016/j.bios.2020.112424>.
- [108] R. Gupta, A. Kumar, S. Kumar, A.K. Pinnaka, N.K. Singhal, Naked eye colorimetric detection of *Escherichia coli* using aptamer conjugated graphene oxide enclosed Gold nanoparticles, *Sensor. Actuator. B Chem.* 329 (2021) 129100, <https://doi.org/10.1016/j.snb.2020.129100>.
- [109] Y. Wei, D. Wang, Y. Zhang, J. Sui, Z. Xu, Multicolor and photothermal dual-readout biosensor for visual detection of prostate specific antigen, *Biosens. Bioelectron.* 140 (2019) 111345, <https://doi.org/10.1016/j.bios.2019.111345>.
- [110] X. Jia, T. Song, Y. Liu, L. Meng, X. Mao, An immunochromatographic assay for carcinoembryonic antigen on cotton thread using a composite of carbon nanotubes and gold nanoparticles as reporters, *Anal. Chim. Acta* 969 (2017) 57–62, <https://doi.org/10.1016/j.aca.2017.02.040>.
- [111] L.L. Meng, T.T. Song, X. Mao, Novel immunochromatographic assay on cotton thread based on carbon nanotubes reporter probe, *Talanta* 167 (2017) 379–384, <https://doi.org/10.1016/j.talanta.2017.02.023>.
- [112] Y. Huang, Y. Wen, K. Baryeh, S. Takalkar, M. Lund, X. Zhang, G. Liu, Magnetized carbon nanotubes for visual detection of proteins directly in whole blood, *Anal. Chim. Acta* 993 (2017) 79–86, <https://doi.org/10.1016/j.aca.2017.09.025>.
- [113] E. Morales-Narváez, A. Merkoçi, Graphene oxide as an optical biosensing platform, *Adv. Mater.* 24 (2012) 3298–3308, <https://doi.org/10.1002/adma.201200373>.
- [114] E. Bozkurt, M. Acar, Y. Onganer, K. Meral, Rhodamine 101-graphene oxide composites in aqueous solution: the fluorescence quenching process of rhodamine 101, *Phys. Chem. Chem. Phys.* 16 (2014) 18276–18281, <https://doi.org/10.1039/c4cp01492h>.
- [115] X. Sun, Y. Lei, Fluorescent carbon dots and their sensing applications, *TrAC Trends Anal. Chem.* (Reference Ed.) 89 (2017) 163–180, <https://doi.org/10.1016/j.trac.2017.02.001>.
- [116] W. Xiang, Z. Zhang, W. Weng, B. Wu, J. Cheng, L. Shi, H. Sun, L. Gao, K. Shi, Highly sensitive detection of carcinoembryonic antigen using copper-free click chemistry on the surface of azide cofunctionalized graphene oxide, *Anal. Chim. Acta* 1127 (2020) 156–162, <https://doi.org/10.1016/j.aca.2020.06.053>.
- [117] M.D. Avila-Huerta, E.J. Ortiz-Riño, D.L. Mancera-Zapata, K. Cortés-Sarabia, E. Morales-Narváez, Facile determination of COVID-19 seroconversion via nonradiative energy transfer, *ACS Sens.* 6 (2021) 2136–2140, <https://doi.org/10.1021/acssensors.1c00795>.
- [118] Y. Liu, A. Kannegulla, B. Wu, L.J. Cheng, Quantum dot fullerene-based molecular beacon nanosensors for rapid, highly sensitive nucleic acid detection, *ACS Appl. Mater. Interfaces* 10 (2018) 18524–18531, <https://doi.org/10.1021/acsami.8b03552>.
- [119] C. Liu, Y. Tang, Y. Chen, J. Deng, W. Li, J. Tang, Ribonuclease H enzyme activity detection based on hybridization chain reaction amplification and graphene oxide nanosheets fluorescence quenching, *J. Nanosci. Nanotechnol.* 20 (2020) 1409–1416, <https://doi.org/10.1166/jnn.2020.17351>.
- [120] C. Wang, C. Wang, J. Qiu, J. Gao, H. Liu, Y. Zhang, L. Han, Ultrasensitive, high-throughput, and rapid simultaneous detection of SARS-CoV-2 antigens and IgG/IgM antibodies within 10 min through an immunoassay biochip, *Microchim. Acta* 188 (2021) 262, <https://doi.org/10.1007/s00604-021-04896-w>.
- [121] O.J. Achadu, K. Takemura, I.M. Khoris, E.Y. Park, Plasmonic/magnetic molybdenum trioxide and graphitic carbon nitride quantum dots-based fluoroimmunosensing system for influenza virus, *Sensor. Actuator. B Chem.* 321 (2020) 128494, <https://doi.org/10.1016/j.snb.2020.128494>.
- [122] L.-D. Xu, J. Zhu, S.-N. Ding, Immunoassay of SARS-CoV-2 nucleocapsid proteins using novel red emission-enhanced carbon dot-based silica spheres, *Analyst* 146 (2021) 5055–5060, <https://doi.org/10.1039/D1AN01010G>.
- [123] I. Khalil, N.M. Julkapli, W.A. Yehye, W.J. Basirun, S.K. Bhargava, Graphene-gold nanoparticles hybrid-synthesis, functionalization, and application in a electrochemical and surface-enhanced Raman scattering biosensor, *Materials* 9 (2016) 406, <https://doi.org/10.3390/ma9060406>.
- [124] N. Soda, B.H.A. Rehm, P. Sonar, N.-T. Nguyen, M.J.A. Shiddiky, Advanced liquid biopsy technologies for circulating biomarker detection, *J. Mater. Chem. B* 7 (2019) 6670–6704, <https://doi.org/10.1039/C9TB01490J>.
- [125] W.A. El-Said, A.S. Al-Bogami, W. Alshitari, Synthesis of gold nanoparticles@ reduced porous graphene-modified ITO electrode for spectroelectrochemical detection of SARS-CoV-2 spike protein, *Spectrochim. Acta Part A Mol. Biomol. Spectrosc.* 264 (2022) 120237, <https://doi.org/10.1016/j.saa.2021.120237>.
- [126] X. Pan, L. Li, H. Lin, J. Tan, H. Wang, M. Liao, C. Chen, B. Shan, Y. Chen, M. Li, A graphene oxide-gold nanostar hybrid based-paper biosensor for label-free SERS detection of serum bilirubin for diagnosis of jaundice, *Biosens. Bioelectron.* 145 (2019) 111713, <https://doi.org/10.1016/j.bios.2019.111713>.
- [127] J. Li, H. Heng, J. Lv, T. Jiang, Z. Wang, Z. Dai, Graphene oxide-assisted and DNA-modulated SERS of AuCu alloy for the fabrication of apurinic/aprimidinic endonuclease I biosensor, *Small* 15 (2019) 1901506, <https://doi.org/10.1002/sml.201901506>.
- [128] J. Lin, X. Chen, P. Huang, Graphene-based nanomaterials for bioimaging, *Adv. Drug Deliv. Rev.* 105 (2016) 242–254, <https://doi.org/10.1016/j.addr.2016.05.013>.
- [129] G. Xu, J. Wang, G. Si, M. Wang, H. Cheng, B. Chen, S. Zhou, Preparation, photoluminescence properties and application for in vivo tumor imaging of curcumin derivative-functionalized graphene oxide composite, *Dyes Pigments* 141 (2017) 470–478, <https://doi.org/10.1016/j.dyepig.2017.02.046>.
- [130] X. Yan, G. Niu, J. Lin, A.J. Jin, H. Hu, Y. Tang, Y. Zhang, A. Wu, J. Lu, S. Zhang, P. Huang, B. Shen, X. Chen, Enhanced fluorescence imaging guided photodynamic therapy of sinoporphyrin sodium loaded graphene oxide, *Biomaterials* 42 (2015) 94–102, <https://doi.org/10.1016/j.biomaterials.2014.11.040>.
- [131] B. Lyu, H.J. Li, F. Xue, L. Sai, B. Gui, D. Qian, X. Wang, J. Yang, Facile, gram-scale and eco-friendly synthesis of multi-color graphene quantum dots by thermal-driven advanced oxidation process, *Chem. Eng. J.* 388 (2020) 124285, <https://doi.org/10.1016/j.cej.2020.124285>.
- [132] C.-C. Fu, C.-Y. Wu, C.-C. Chien, T.-H. Hsu, S.-F. Ou, S.-T. Chen, C.-H. Wu, C.-T. Hsieh, R.-S. Juang, Y.-H. Hsueh, Polyethylene Glycol₆₀₀₀/carbon nanodots as fluorescent bioimaging agents, *Nanomaterials* 10 (2020) 677, <https://doi.org/10.3390/nano10040677>.
- [133] M. Yudasaka, Y. Yomogida, M. Zhang, M. Nakahara, N. Kobayashi, T. Tanaka, Y. Okamoto-Ogura, K. Saeki, H. Kataura, Fasting-dependent vascular permeability enhancement in brown adipose tissues evidenced by using carbon nanotubes as fluorescent probes, *Sci. Rep.* 8 (2018) 14446, <https://doi.org/10.1038/s41598-018-32758-8>.
- [134] S. Diao, J.L. Blackburn, G. Hong, A.L. Antaris, J. Chang, J.Z. Wu, B. Zhang, K. Cheng, C.J. Kuo, H. Dai, Fluorescence imaging *in vivo* at wavelengths beyond 1500 nm, *Angew. Chem. Int. Ed.* 54 (2015) 14758–14762, <https://doi.org/10.1002/anie.201507473>.
- [135] J.M. Yoo, J.H. Kang, B.H. Hong, Graphene-based nanomaterials for versatile imaging studies, *Chem. Soc. Rev.* 44 (2015) 4835–4852, <https://doi.org/10.1039/c5cs00072f>.
- [136] W.S. Kuo, C.Y. Chang, K.S. Huang, J.C. Liu, Y.T. Shao, C.H. Yang, P.C. Wu, Amino-functionalized nitrogen-doped graphene-quantum-dot-based nanomaterials with nitrogen and amino-functionalized group content dependence for highly efficient

- two-photon bioimaging, *Int. J. Mol. Sci.* 21 (2020), <https://doi.org/10.3390/ijms21082939>.
- [137] Z. Luo, D. Yang, C. Yang, X. Wu, Y. Hu, Y. Zhang, L. Yuwen, E.K.L. Yeow, L. Weng, W. Huang, L. Wang, Graphene quantum dots modified with adenine for efficient two-photon bioimaging and white light-activated antibacteria, *Appl. Surf. Sci.* 434 (2018) 155–162, <https://doi.org/10.1016/j.apsusc.2017.10.121>.
- [138] X. Qin, Y. Si, D. Wang, Z. Wu, J. Li, Y. Yin, Nanoconjugates of Ag/Au/Carbon nanotube for alkyne-mediated ratiometric SERS imaging of hypoxia in hepatic ischemia, *Anal. Chem.* 91 (2019) 4529–4536, <https://doi.org/10.1021/acs.analchem.8b05487>.
- [139] N. Bugárová, A. Annušová, M. Bodík, P. Šiffalovič, M. Labudová, I. Kajanová, M. Zatošičová, S. Pastoreková, E. Majkóvá, M. Omastová, Molecular targeting of bioconjugated graphene oxide nanocarriers revealed at a cellular level using label-free Raman imaging, *Nanomed. Nanotechnol. Biol. Med.* 30 (2020) 102280, <https://doi.org/10.1016/j.nano.2020.102280>.
- [140] C. Enzinger, F. Barkhof, O. Ciccarelli, M. Filippi, L. Kappos, M.A. Rocca, S. Ropele, À. Rovira, T. Schneider, N. de Stefano, H. Vrenken, C. Wheeler-Kingshott, J. Wuerfel, F. Fazekas, Nonconventional MRI and microstructural cerebral changes in multiple sclerosis, *Nat. Rev. Neurol.* 11 (2015) 676–686, <https://doi.org/10.1038/nrneurol.2015.194>.
- [141] C. Yan, C. Chen, L. Hou, H. Zhang, Y. Che, Y. Qi, X. Zhang, J. Cheng, Z. Zhang, Single-walled carbon nanotube-loaded doxorubicin and Gd-DTPA for targeted drug delivery and magnetic resonance imaging, *J. Drug Target.* 25 (2017) 163–171, <https://doi.org/10.1080/1061186X.2016.1221958>.
- [142] S.E. Moghaddam, M. Hernández-Rivera, N.G. Zaibac, A. Ajala, M. da Graça Cabreira-Hansen, S. Mowlazadeh-Haghighi, J.T. Willerson, E.C. Perin, R. Muthupillai, L.J. Wilson, A new high-performance gadonanotube-polymer hybrid material for stem cell labeling and tracking by MRI, *Contrast Media Mol. Imaging* (2018) 1–8, <https://doi.org/10.1155/2018/2853736>, 2018.
- [143] H. Wang, R. Revia, Q. Mu, G. Lin, C. Yen, M. Zhang, Single-layer boron-doped graphene quantum dots for contrast-enhanced: *in vivo* T₁-weighted MRI, *Nanoscale Horiz* 5 (2020) 573–579, <https://doi.org/10.1039/c9nh00608g>.
- [144] Y. Peng, C. Ye, R. Yan, Y. Lei, D. Ye, H. Hong, T. Cai, Activatable core-shell metallofullerene: an efficient nanoplatfor for bimodal sensing of glutathione, *ACS Appl. Mater. Interfaces* 11 (2019) 46637–46644, <https://doi.org/10.1021/acsami.9b18807>.
- [145] M.L. Chen, Z.W. Gao, X.M. Chen, S.C. Pang, Y. Zhang, Laser-assisted *in situ* synthesis of graphene-based magnetic-responsive hybrids for multimodal imaging-guided chemo/photothermal synergistic therapy, *Talanta* 182 (2018) 433–442, <https://doi.org/10.1016/j.talanta.2018.02.030>.
- [146] M. Zhang, W. Wang, Y. Cui, N. Zhou, J. Shen, Near-infrared light-mediated photodynamic/photothermal therapy nanoplatfor by the assembly of Fe₃O₄ carbon dots with graphitic black phosphorus quantum dots, *Int. J. Nanomed.* 13 (2018) 2803–2819, <https://doi.org/10.2147/IJN.S156434>.
- [147] H. Ge, P.J. Riss, V. Mirabello, D.G. Calatayud, S.E. Flower, R.L. Arrowsmith, T.D. Fryer, Y. Hong, S. Sawiak, R.M.J. Jacobs, S.W. Botchway, R.M. Tyrrell, T.D. James, J.S. Fossey, J.R. Dilworth, F.I. Aigbirhio, S.I. Pascu, Behavior of supramolecular assemblies of radiometal-filled and fluorescent carbon nanocapsules *in vitro* and *in vivo*, *Inside Cell.* 3 (2017) 437–460, <https://doi.org/10.1016/j.jchempr.2017.06.013>.
- [148] Y. Peng, D. Yang, W. Lu, X. Hu, H. Hong, T. Cai, Positron emission tomography (PET) guided glioblastoma targeting by a fullerene-based nanoplatfor with fast renal clearance, *Acta Biomater.* 61 (2017) 193–203, <https://doi.org/10.1016/j.actbio.2017.08.011>.
- [149] T. Cao, X. Zhou, Y. Zheng, Y. Sun, J. Zhang, W. Chen, J. Zhang, Z. Zhou, S. Yang, Y. Zhang, H. Yang, M. Wang, Chelator-free conjugation of ^{99m}Tc and Gd³⁺ to PEGylated nanographene oxide for dual-modality SPECT/MR imaging of lymph nodes, *ACS Appl. Mater. Interfaces* 9 (2017) 42612–42621, <https://doi.org/10.1021/acsami.7b14836>.
- [150] A.B.E. Attia, G. Balasundaram, M. Moothanchery, U.S. Dinis, R. Bi, V. Ntziachristos, M. Olivo, A review of clinical photoacoustic imaging: current and future trends, *Photoacoustics* 16 (2019) 100144, <https://doi.org/10.1016/j.pacs.2019.100144>.
- [151] L. Nie, X. Chen, Structural and functional photoacoustic molecular tomography aided by emerging contrast agents, *Chem. Soc. Rev.* 43 (2014) 7132–7170, <https://doi.org/10.1039/c4cs00086b>.
- [152] A.D. la Zerdá, Z. Liu, S. Bodapati, R. Teed, S. Vaithilingam, B.T. Khuri-Yakub, X. Chen, H. Dai, S.S. Gambhir, Ultrahigh sensitivity carbon nanotube agents for photoacoustic molecular imaging in living mice, *Nano Lett.* 10 (2010) 2168–2172, <https://doi.org/10.1021/nl100890d>.
- [153] A.R. Genady, D. Fong, S.R. Slikboer, M.E. El-Zaria, R. Swann, N. Janzen, A. Faraday, S.A. McNelles, M. Rezvani, S. Sadeghi, A. Adronov, J.F. Valliant, ^{99m}Tc-functionalized single-walled carbon nanotubes for bone targeting, *ACS Appl. Mater. Interfaces* 3 (2020) 11819–11824, <https://doi.org/10.1021/acsanm.0c02339>.
- [154] M. Chen, S. Tang, Z. Guo, X. Wang, S. Mo, X. Huang, G. Liu, N. Zheng, Core-shell Pd@Au nanoplates as theranostic agents for *in-vivo* photoacoustic imaging, CT imaging, and photothermal therapy, *Adv. Mater.* 26 (2014) 8210–8216, <https://doi.org/10.1002/adma.201404013>.
- [155] Y. Xuan, R.Y. Zhang, D.H. Zhao, X.S. Zhang, J. An, K. Cheng, X.L. Hou, X.L. Song, Y. di Zhao, X.Q. Yang, Ultrafast synthesis of gold nanosphere cluster coated by graphene quantum dot for active targeting PA/CT imaging and near-infrared laser/pH-triggered chemo-photothermal synergistic tumor therapy, *Chem. Eng. J.* 369 (2019) 87–99, <https://doi.org/10.1016/j.cej.2019.03.035>.
- [156] H. Wang, H. Wang, X. Duan, Y. Sun, X. Wang, Z. Li, Highly sensitive and multiplexed quantification of mRNA splice variants by the direct ligation of DNA probes at the exon junction and universal PCR amplification, *Chem. Sci.* 8 (2017) 3635–3640, <https://doi.org/10.1039/c7sc00094d>.
- [157] H. Deng, Z. Gao, Bioanalytical applications of isothermal nucleic acid amplification techniques, *Anal. Chim. Acta* 853 (2015) 30–45, <https://doi.org/10.1016/j.aca.2014.09.037>.
- [158] X. Liu, F. Wang, R. Aizen, O. Yehezkeili, I. Willner, Graphene oxide/nucleic-acid-stabilized silver nanoclusters: functional hybrid materials for optical aptamer sensing and multiplexed analysis of pathogenic DNAs, *J. Am. Chem. Soc.* 135 (2013) 11832–11839, <https://doi.org/10.1021/ja403485r>.
- [159] S. Jeong, E. González-Grandío, N. Navarro, R.L. Pinals, F. Ledesma, D. Yang, M.P. Landry, Extraction of viral nucleic acids with carbon nanotubes increases SARS-CoV-2 quantitative reverse transcription polymerase chain reaction detection sensitivity, *ACS Nano* 15 (2021) 10309–10317, <https://doi.org/10.1016/acsnano.1c02494>.
- [160] Y. Wang, F. Wang, H. Wang, M. Song, Graphene oxide enhances the specificity of the polymerase chain reaction by modifying primer-template matching, *Sci. Rep.* 7 (2017), <https://doi.org/10.1038/s41598-017-16836-x>.
- [161] C. Hu, Z. Yang, Z. Song, L. Xiao, Y. He, A strategy for preparing non-fluorescent graphene oxide quantum dots as fluorescence quenchers in quantitative real-time PCR, *RSC Adv.* 10 (2020), <https://doi.org/10.1039/d0ra00142b>, 14944–14952.
- [162] C. Hu, L. Zhang, Z. Yang, Z. Song, Q. Zhang, Y. He, Graphene oxide-based qRT-PCR assay enables the sensitive and specific detection of miRNAs for the screening of ovarian cancer, *Anal. Chim. Acta* 1174 (2021) 338715, <https://doi.org/10.1016/j.aca.2021.338715>.
- [163] J.W. Kim, M. Kim, K.K. Lee, K.H. Chung, C.S. Lee, Effects of graphene oxide-gold nanoparticles nanocomposite on highly sensitive foot-and-mouth disease virus detection, *Nanomaterials* 10 (2020) 1–10, <https://doi.org/10.3390/nano10101921>.
- [164] H. Li, J. Huang, J. Lv, H. An, X. Zhang, Z. Zhang, C. Fan, J. Hu, Nanoparticle PCR: nanogold-assisted PCR with enhanced specificity, *Angew. Chem. Int. Ed.* 44 (2005) 5100–5103, <https://doi.org/10.1002/anie.200500403>.
- [165] Q. Wu, H.K. Kang, B.N. Oh, J. Kim, Size-dependent interactions between Au Nanoparticles and DNA in electrochemical oxidation by metal complexes, *J. Phys. Chem. C* 116 (2012) 8020–8026, <https://doi.org/10.1021/jp209470g>.
- [166] S. Jung, J. Kim, J. Kim, S.H. Yang, S.K. Kim, Extensible multiplex real-time PCR for rapid bacterial identification with carbon nanotube composite microparticles, *Biosens. Bioelectron.* 94 (2017) 256–262, <https://doi.org/10.1016/j.bios.2017.02.049>.
- [167] R. Cai, S. Zhang, L. Chen, M. Li, Y. Zhang, N. Zhou, Self-assembled DNA nanoflowers triggered by a DNA walker for highly sensitive electrochemical detection of *Staphylococcus aureus*, *ACS Appl. Mater. Interfaces* 13 (2021) 4905–4914, <https://doi.org/10.1021/acsami.0c22062>.
- [168] Y. Wang, X. Shang, J. Liu, Y. Guo, ATP mediated rolling circle amplification and opening DNA-gate for drug delivery to cell, *Talanta* 176 (2018) 652–658, <https://doi.org/10.1016/j.talanta.2017.08.087>.
- [169] Q. Lin, X. Ye, Z. Huang, B. Yang, X. Fang, H. Chen, J. Kong, Graphene oxide-based suppression of nonspecificity in loop-mediated isothermal amplification enabling the sensitive detection of cyclooxygenase-2 mRNA in colorectal cancer, *Anal. Chem.* 91 (2019) 15694–15702, <https://doi.org/10.1021/acs.analchem.9b03861>.
- [170] M.H. Choi, J. Lee, Y.J. Seo, Combined recombinase polymerase amplification/rkDNA–graphene oxide probing system for detection of SARS-CoV-2, *Anal. Chim. Acta* 1158 (2021) 338390, <https://doi.org/10.1016/j.aca.2021.338390>.
- [171] M. Giannetto, M.V. Bianchi, M. Mattarozzi, M. Careri, Competitive amperometric immunosensor for determination of p53 protein in urine with carbon nanotubes/gold nanoparticles screen-printed electrodes: a potential rapid and noninvasive screening tool for early diagnosis of urinary tract carcinoma, *Anal. Chim. Acta* 991 (2017) 133–141, <https://doi.org/10.1016/j.aca.2017.09.005>.
- [172] D.C. Marcano, D.v. Kosynkin, J.M. Berlin, A. Sinitskii, Z. Sun, A. Slesarev, L.B. Alemany, W. Lu, J.M. Tour, Improved synthesis of graphene oxide, *ACS Nano* 4 (2010) 4806–4814, <https://doi.org/10.1021/nl1006368>.
- [173] K. Kim, M.J. Kim, D.W. Kim, S.Y. Kim, S. Park, C.B. Park, Clinically accurate diagnosis of Alzheimer's disease via multiplexed sensing of core biomarkers in human plasma, *Nat. Commun.* 11 (2020) 1–9, <https://doi.org/10.1038/s41467-019-13901-z>.
- [174] M. Yang, M. Zhang, Biodegradation of carbon nanotubes by macrophages, *Front. Mater.* 6 (2019), <https://doi.org/10.3389/fmats.2019.00225>.
- [175] M. Chen, X. Qin, G. Zeng, Biodegradation of carbon nanotubes, graphene, and their derivatives, *Trends Biotechnol.* 35 (2017) 836–846, <https://doi.org/10.1016/j.tibtech.2016.12.001>.
- [176] B. Ma, C. Martín, R. Kurapati, A. Bianco, Degradation-by-design: how chemical functionalization enhances the biodegradability and safety of 2D materials, *Chem. Soc. Rev.* 49 (2020) 6224–6247, <https://doi.org/10.1039/C9CS00822E>.
- [177] R. Kurapati, J. Russier, M.A. Squillaci, E. Treossi, C. Ménard-Moyon, A.E. del Rio-Castillo, E. Vazquez, P. Samorì, V. Palermo, A. Bianco, Dispersibility-dependent biodegradation of graphene oxide by myeloperoxidase, *Small* 11 (2015) 3985–3994, <https://doi.org/10.1002/sml.201500038>.